Science of the Total Environment

A Framework for Drought Monitoring and Assessment from a Drought Propagation Perspective under Non-stationary Environments

--Manuscript Draft--

Manuscript Number:	STOTEN-D-24-23771
Article Type:	Research Paper
Keywords:	Nonstationary Integrated Drought Index; Nonstationary marginal distributions; D-vine copula; Large-scale climate pattern; Anthropogenic influences
Corresponding Author:	xinyu wu Dalian University of Technology CHINA
First Author:	Xingchen Wei
Order of Authors:	Xingchen Wei
	Xinyu Wu
	Hongbo Zhang
	Tian Lan
	Chuntian Cheng
	Yanrui Wu
	George Aggidis
Abstract:	According to the coupled influence of climate variation and anthropogenic activities, hydro-meteorological variables are hard to keep stationary in a changing environment. Consequently, the efficacy of traditional standardized drought indices, predicated upon the assumption of stationarity, has been called into question. In China, the challenge of drought monitoring and declaration is exacerbated by the need for multiple drought indices covering meteorological, agricultural, hydrological, and groundwater aspects, often lacking real-time availability. To address these challenges, we developed a framework for drought monitoring and assessment from a drought propagation perspective. Central to this is the Nonstationary Integrated Drought Index (NIDI), which integrates responses from meteorological, agricultural, hydrological, and groundwater droughts, accounting for climate change and anthropogenic influences. First, we analyse the process of drought propagation to select the suitable time scale standardized drought index. Subsequently, significant large-scale climatic indices are selected through linear and nonlinear correlation analyses to identify climate anomalies. Anthropogenic influences are assessed using indicators such as the Normalized Difference Vegetation Index (NDVI), Impervious Surface Ratio (ISR), and population density (POP). Nonstationary probability models are then developed for precipitation, soil moisture, runoff, and groundwater series, incorporating climatic and human-induced factors. Finally, the NIDI is calculated using a D-vine copula model, with parameter estimation and updating facilitated by a genetic algorithm, representing the temporal dependence structure among the variables. A case study in the Hulu River Basin of western China validated the NIDI. Results showed that the NIDI effectively accounts for nonstationary hydro-meteorological variables due to climate change and human activities, accurately reproducing their time-dependent structure. Compared to conventional indices like SPI, SSI, SRI, and SGI, the NIDI identifies more extreme drought events. In conclusion, the presented NIDI offers a more comprehensive approach to drought identification, providing valuable insights for accurate drought detection and effective drought-related policy-making.
Suggested Reviewers:	Shengzhi Huang huangshengzhi7788@126.com
	Kairong Lin linkr@mail.sysu.edu.cn
	Lei Gu

	shisan@hust.edu.cn
	Chong-yu Xu c.y.xu@geo.uio.no
	Yongqin David Chen ydavidchen@cuhk.edu.cn
	wenchuan wang wangwenchuan@ncwu.edu.cn
Opposed Reviewers:	

June 6, 2024

Dear Editor,

We wish to submit a revised manuscript entitled "**A Framework for Drought Monitoring and Assessment from a Drought Propagation Perspective under Non-stationary Environments**" for consideration by ***Science of The Total Environment***. We confirm that this work is original and has not been published elsewhere, nor is it currently under consideration for publication elsewhere. All authors have read and approved the manuscript being submitted, and agree to its submittal to this journal, and have no conflicts of interest to disclose.

In China, the challenge of drought monitoring and declaration is exacerbated by the need for multiple drought indices covering meteorological, agricultural, hydrological, and groundwater aspects, often lacking real-time availability. Especially in the context of changing environments and the non-stationarity of hydro-meteorological variables. Even though the importance of developing a multivariate nonstationary drought index that considers the environmental change has been recognized, relevant research remains rare. To address these challenges, we develop a framework for drought monitoring and assessment from a drought propagation perspective. Central to this is our proposed a Nonstationary Integrated Drought Index (NIDI) that combines the response of meteorological, agricultural, hydrological and groundwater droughts, while accounting for the influences of climate change and anthropogenic activities. To validate the applicability and effectiveness of the NIDI, we conducted a case study in the Hulu River Basin of western China. The results demonstrate that the NIDI successfully accounts for nonstationary hydro-meteorological variables associated with climate change and human activities, accurately reproducing their time-dependent structure. In conclusion, the presented NIDI offers a more comprehensive approach to drought identification, providing valuable insights for accurate drought detection and effective drought-related policy-making.

Highlights of this paper:

1. An integrated framework is developed for drought monitoring and assessment from a drought propagation perspective under non-stationary environments.
2. A novel Nonstationary Integrated Drought Index (NIDI) based on meteorological, agricultural, hydrological and groundwater droughts is proposed to detect and extract drought features.
3. The NIDI uses SPI, SRI, SSI, and SGI by incorporating the response of precipitation, soil moisture, runoff, and groundwater.
4. The NIDI is calculated by a time-varying nonstationary joint probability model with climate-driven and human-induced factors as explanatory variables.

Thank you for your consideration of this manuscript.

Sincerely,

Xinyu Wu

Corresponding author: X. Y. Wu Prof/Ph.D. E-mail: wuxinyu@dlut.edu.cn

Title: A Framework for Drought Monitoring and Assessment from a Drought Propagation Perspective under Non-stationary Environments

Xingchen Wei: Methodology, Software, Visualization, Writing - original draft. Xinyu Wu: Conceptualization, Software, Funding acquisition, Supervision, Resources. Hongbo Zhang: Writing - review & editing. Tian Lan: Data curation, Funding acquisition, Formal analysis. Chuntian Cheng: Supervision. Yanrui Wu: Software. George Aggidis: Investigation.

Author names and affiliations:

1. Xingchen Wei, Ph.D. Student, Institute of Hydropower and Hydroinformatics, Dalian University of Technology, Dalian 116024, China. Key Laboratory of Ocean Energy Utilization and Energy Conservation of Ministry of Education, Dalian University of Technology, Dalian 116024, China. Email: xingchenwei@mail.dlut.edu.cn

2. Xinyu Wu, Professor, Institute of Hydropower and Hydroinformatics, Dalian University of Technology, Dalian 116024, China. Key Laboratory of Ocean Energy Utilization and Energy Conservation of Ministry of Education, Dalian University of Technology, Dalian 116024, China. Email: wuxinyu@dlut.edu.cn

3. Hongbo Zhang, Professor, School of Water and Environment, Chang'an University, Xi'an, 710054, China. Key Laboratory of Subsurface Hydrology and Ecological Effect in Arid Region, Ministry of Education, Chang'an University, Xi'an, 710054, China. Email: hbzhang@chd.edu.cn

4. Tian Lan, Lecturer, School of Water and Environment, Chang'an University, Xi'an, 710054, China. Key Laboratory of Subsurface Hydrology and Ecological Effect in Arid Region, Ministry of Education, Chang'an University, Xi'an, 710054, China. Email: tianlan@chd.edu.cn

5. Chuntian Cheng, Professor, Institute of Hydropower and Hydroinformatics, Dalian University of Technology, Dalian 116024, China. Key Laboratory of Ocean Energy Utilization and Energy Conservation of Ministry of Education, Dalian University of Technology, Dalian 116024, China. Email: ctcheng@dlut.edu.cn

6. Yanrui Wu, Engineer, Shandong Survey and Design Institute of Water Conservancy Co., Ltd, Jinan, 250001, China. Email: wuyanrui12345@163.com

7. George Aggidis, Professor, School of Engineering, Lancaster University, Lancaster, LA1 4YR, United Kingdom, Email: g.aggidis@lancaster.ac.uk

Corresponding author:

Xinyu Wu, Professor, Institute of Hydropower and Hydroinformatics, Dalian University of Technology, Dalian 116024, China. Key Laboratory of Ocean Energy Utilization and Energy Conservation of Ministry of Education, Dalian University of Technology, Dalian 116024, China. Email: wuxinyu@dlut.edu.cn

Graphical Abstract

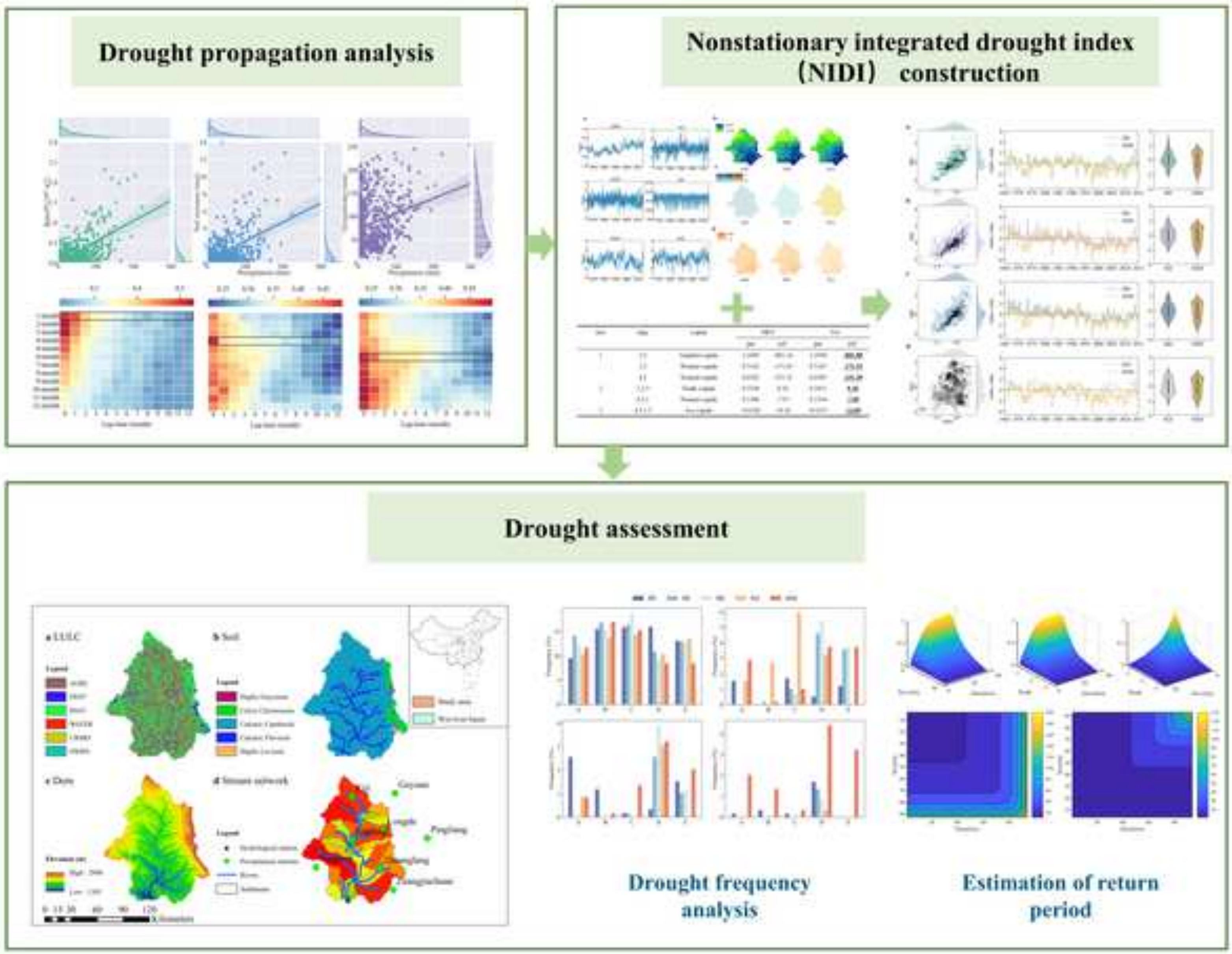

Highlights of this paper:

1. An integrated framework is developed for drought monitoring and assessment from a drought propagation perspective under non-stationary environments.
2. A novel Nonstationary Integrated Drought Index (NIDI) based on meteorological, agricultural, hydrological and groundwater droughts is proposed to detect and extract drought features.
3. The NIDI uses SPI, SRI, SSI, and SGI by incorporating the response of precipitation, soil moisture, runoff, and groundwater.
4. The NIDI is calculated by a time-varying nonstationary joint probability model with climate-driven and human-induced factors as explanatory variables.

A Framework for Drought Monitoring and Assessment from a Drought Propagation Perspective under Non-stationary Environments

Xingchen Wei[1,2], Xinyu Wu[1,2], Hongbo Zhang[3,4,5], Tian Lan[3,4,5], Chuntian Cheng[1,2], Yanrui Wu[6], George Aggidis[7]

[1]Institute of Hydropower and Hydroinformatics, Dalian University of Technology, Dalian 116024, China.
[2]Key Laboratory of Ocean Energy Utilization and Energy Conservation of Ministry of Education, Dalian University of Technology, Dalian, 116024, China
[3]School of Water and Environment, Chang'an University, Xi'an, 710054, China.
[4]Key Laboratory of Subsurface Hydrology and Ecological Effects in Arid Region of the Ministry of Education, Chang'an University, Xi'an 710054, China.
[5]Key Laboratory of Eco-Hydrology and Water Security in Arid and Semi-Arid Regions of Ministry of Water Resources, Chang'an University, Xi'an 710054, China.
[6]Engineer of Shandong Survey and Design Institute of Water Conservancy Co., Ltd, Jinan, 250001, China.
[7]School of Engineering, Lancaster University, Lancaster, LA1 4YR, United Kingdom

Correspondence to: Xinyu Wu (wuxinyu@dlut.edu.cn)

Abstract. According to the coupled influence of climate variation and anthropogenic activities, hydro-meteorological variables are hard to keep stationary in a changing environment. Consequently, the efficacy of traditional standardized drought indices, predicated upon the assumption of stationarity, has been called into question. In China, the challenge of drought monitoring and declaration is exacerbated by the need for multiple drought indices covering meteorological, agricultural, hydrological, and groundwater aspects, often lacking real-time availability. To address these challenges, we developed a framework for drought monitoring and assessment from a drought propagation perspective. Central to this is the Nonstationary Integrated Drought Index (NIDI), which integrates responses from meteorological, agricultural, hydrological, and groundwater droughts, accounting for climate change and anthropogenic influences. First, we analyse the process of drought propagation to select the suitable time scale standardized drought index. Subsequently, significant large-scale climatic indices are selected through linear and nonlinear correlation analyses to identify climate anomalies. Anthropogenic influences are assessed using indicators such as the Normalized Difference Vegetation Index (NDVI), Impervious Surface Ratio (ISR), and population density (POP). Nonstationary probability models are then developed for precipitation, soil moisture, runoff, and groundwater series, incorporating climatic and human-induced factors. Finally, the NIDI is calculated using a D-vine copula model, with parameter estimation and updating facilitated by a genetic algorithm, representing the temporal dependence structure among the variables. A case study in the Hulu River Basin of western China validated the NIDI. Results showed that the NIDI effectively accounts for nonstationary hydro-meteorological variables due to climate change and human activities, accurately reproducing their time-dependent structure. Compared to conventional indices like SPI, SSI, SRI, and SGI, the NIDI identifies more extreme drought events. In conclusion, the presented NIDI offers a more comprehensive approach to drought identification, providing valuable insights for accurate drought detection and effective drought-related policy-making.

Keywords: Nonstationary Integrated Drought Index, Nonstationary marginal distributions, D-vine copula, Large-scale climate pattern, Anthropogenic influences

1 Introduction

Drought, one of the most disruptive natural hazards, dramatically affects the spatial-temporal pattern of water and heat on regional or even global scales (Liu et al., 2017; Zhao et al., 2017). Severe droughts have far-reaching consequences, particularly in developing countries, where they exacerbate existing vulnerabilities and trigger a cascade of socio-economic challenges (Shah and Mishra, 2020). China is the largest developing country, suffering from severe drought. The most severe drought always happened in most northwest, southwest, and southeast areas of China (Shao et al., 2022). Consequently, it is crucial to cope with the drought problems. Generally, drought monitoring and water resource management plans were the dominating way to answer the challenge of severe drought problems. Drought indices are powerful tools for monitoring and determining drought severity. However, the accuracy of drought assessment is becoming increasingly complex due to the non-stationary nature of hydro-meteorological variables. Traditional drought indices, which often rely on the assumption of stationarity, may not be fully reliable in the context of ongoing climate change and the significant influence of human activities (Shao et al., 2022). Therefore, it is urgent to propose a novel approach for regional and even global drought assessment and management.

As one of the most complex phenomena, drought is notoriously hard to define (Shah and Mishra, 2020; Svensson et al., 2017). It can be associated with water shortages, the greenness of vegetation, and a deficiency in rainfall, streamflow, soil moisture, even socioeconomic conditions (Zargar et al., 2011; Mishra and Singh, 2010). According to the water cycle and different types of water deficits, drought broadly can be summarized into four main categories: meteorological, agricultural, hydrological and socioeconomic droughts (Zargar et al., 2011; Heim, 2002). In addition, drought typically begins with sustained periods of below-average precipitation, known as meteorological drought, and progresses to inadequate surface and/or groundwater supplies (hydrological drought), which further triggers agricultural and socioeconomic droughts (Dracup et al., 1980). Therefore, meteorological, agricultural, hydrological and groundwater droughts deserve sufficient consideration.

In recent decades, there has been a surge in the development of various drought indices aimed at enhancing drought monitoring and mitigating associated risks. These indices serve as crucial tools for assessing drought severity, duration, and spatial extent, providing valuable insights for decision-makers and stakeholders involved in drought management and response efforts (Yin et al., 2018; Liu et al., 2017). The standardized drought indices based on probability distribution functions, have been broadly used for meteorological and hydrological droughts assessment, including the Standardized Precipitation Index (McKee et al., 1993), the Standardized Runoff Index (Shukla and Wood, 2008), the Standardized stream index (Shukla and Wood, 2008), and the Standardized Soil moisture Index (AghaKouchak, 2014). The above wildly used indices are dependent on a sole hydro-meteorological variable (e.g., precipitation, runoff, or soil moisture) (Huang et al., 2016). However, various hydro-meteorological variables have inconsistent changes and complicated physical interactions among direct (Zhang et al., 2021). Thus, the a-single-variable-based drought indices are insufficient for dependable drought risk evaluation and sensible decision-making.

To overcome this shortcoming, a variety of drought indices that incorporate multiple hydro-meteorological factors were proposed (Zhang et al., 2021; Rajsekhar et al., 2015). For instance, Hao and AghaKouchak (2013) introduced the Multivariate Standardized Drought Index (MSDI), which combines the precipitation and soil moisture content via copula. Rajsekhar et al. (2015) developed a multivariate drought index (MDI) to detect drought conditions via entropy theory and multiple hydro-meteorological variables. Shah and Mishra (2020) proposed an Integrated Drought Index (IDI) that characterized three droughts: hydrology, meteorology, and agriculture, and accounted for groundwater storage at the same time. Won et al. (2020) developed a Copula-based Joint Drought Index (CJDI) to measure droughts in terms of atmospheric moisture supply and demand simultaneously. Li et al. (2021) constructed a bivariate combined drought index (BCDIbcf) to describe meteorological and hydrological droughts comprehensively. In general, these standardized drought indices were proposed according to the hypothesis of stationarity. Moreover, they are calculated by hydro-meteorological variables with a statistically stationary distribution. Nevertheless, hydro-meteorological variables vary significantly with time based on previous research (Shao et al., 2022). Furthermore, non-stationarity will exist in many regions of this world which combine impacts of climate variability and human activities (Strupczewski et al., 2001). Thus, the effectiveness and applicability of traditional standardized drought indices based on the stationarity assumption have been questioned in a changing environment.

Climate variation and anthropogenic activities are two main driving forces that affect the hydrological cycle and its available water resources, resulting in more frequent and extensive terrestrial extreme phenomena such as droughts (2020; Lan et al., 2020; Dai, 2013; Sheffield et al., 2012). Generally, climate variation can be traced to large-scale climate patterns, such as the El Niño Southern Oscillation (ENSO), the Pacific Decadal Oscillation (PDO), and the Arctic Oscillation (AO) (Yu et al., 2019; Frazier et al., 2018). It seems reasonable to represent the nonstationary climate anomalies by the dependence of hydro-meteorological variables on large-scale climate patterns (Forootan et al., 2019; Ndehedehe et al., 2019). In addition to climate change, scholars have made various efforts to represent anthropogenic impacts in the hydrology community (Chen et al., 2019; Zhang et al., 2018). One of the widely used ways to present human activities is the hydrological model (Zhang et al., 2012). In recent years, numerous studies have explained the non-stationarity of droughts via proposed nonstationary drought indices with climate and human-induced indices. Li et al. (2015) introduced a Nonstationary Standardized Precipitation Index (NSPI), which incorporated climate change into the meteorological drought index. Wang et al. (2020) developed the Nonstationary Standardized Streamflow Index (NSSI), which depicts the non-stationarity in streamflow by utilizing climatic and human-induced indices as explanatory variables. Zhang et al. (2021) proposed a nonstationary meteorological and hydrological drought index (NMHDI), taking anthropogenic impacts on runoff into account, which provides valuable information for drought management. Shao et al. (2022) proposed a nonstationary standardized runoff index (NSRI) based on GAMLSS, considering climate variation and human activity influence, which detected more frequent severe and extreme droughts.

In the above-mentioned studies, nonstationary drought models showed improved performance in reproducing extreme droughts when compared to those based on stationarity assumptions. Therefore, the nonstationary drought indices have an excellent advantage in drought risk monitoring and assessment. Nevertheless, drought phenomena are related to multiple hydro-meteorological variables. Thus, these indices derived from a single hydro-meteorological variable would be insufficient for an overall idea of the drought condition and further drought management (Rajsekhar et al., 2015; Hao and AghaKouchak, 2013). Meanwhile, few studies have considered the climatic and anthropogenic impacts of drought from a comprehensive perspective. Even though the importance of developing a multivariate nonstationary drought index that considers the environmental change has been recognized, relevant research remains rare (Song et al., 2020).

To address the aforementioned challenges and explore comprehensive methods for monitoring and assessing drought events under climate change, it is necessary to concretely analyse the impacts of climate change factors and human activities on hydro-meteorological variables. This entails employing nonstationary probability models to characterize the response of hydro-meteorological variables to these factors accurately, thereby enabling precise drought monitoring and assessment. The proposed method can provide valuable guidance for the water resources management in non-stationary environments. The objective of this study is to develop a framework for construct a comprehensive framework for monitoring and assessing drought under non-stationary environments. The paper focuses on three main aspects:

- Developing an integrated framework for monitoring and assessing drought events from a drought propagation perspective under non-stationary environments.
- Proposing a novel Nonstationary Integrated Drought Index (NIDI) to detect the drought events and extract drought features.
- Assessing drought risk via NIDI and frequency analysis methods, and exploring the response patterns of drought to climate change and human activities.

To achieve these objectives, this study selected the Hulu River Basin to illustrate our research objectives and methods. The remainder of the paper is organized as follows. Section 2 describes the research basins. Section 3 introduces the methodology and details of the analysis approaches. The key results and discussion are presented in Sections 4 and 5. Section 6 exhibits the main conclusions of this study. The results could support a new perspective to construct recent comprehensive nonstationary drought indices under a changing climate. It can provide valuable references for accurate drought detection and effective drought-related policy-making.

2 Study Case and data description

2.1 Case study area

The Hulu River serves as the primary tributary in the upper reaches of the Wei River, as illustrated in Figure 1. Originating from Moon Mountain in Xi Ji county, China, the Hulu River plays a crucial role in the hydrological network of the region, contributing to the overall water resources and ecological balance. This basin is located between 34°30′ to 36°30′ northern longitudes and 105°05′ to 106°30′ eastern latitudes. It covers an area of the catchment above the Qin'an station nearly 9805 km^2 (Han et al., 2020), and locates in the Loess Plateau region. The Hulu River Basin experiences a moderate continental monsoon climate. The features include a cold winter with minimal snowfall, a hot and rainy summer, and quickly cool autumn. The main type of land use in the Hulu River Basin includes Cropland (AGRL), forestland (FRST), grassland (PAST), water bodies (WATR), residential areas (URMD), and unused land (SWRN) (Figure 1a).

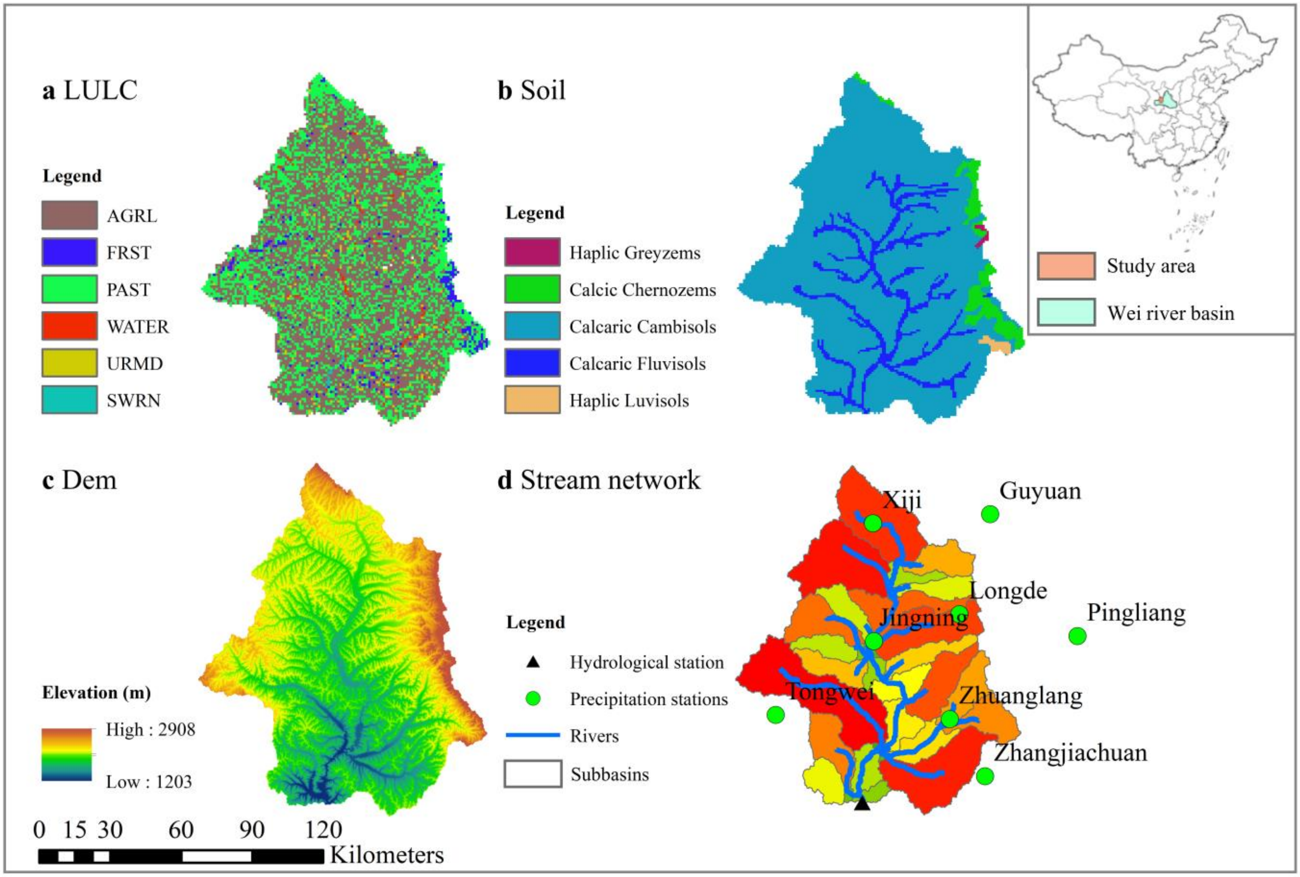

Figure 1. Basic information related to **a,** land use/land cover, **b,** soil, **c,** digital elevation model (DEM), **d,** stream network and observation stations for Hulu River basin, western China

In recent years, the hydro-meteorological variables within the Hulu River Basin have undergone significant changes, driven by the combined impacts of climate change and human activities. This is because climate change directly affects the formation of runoff processes, while human activities mainly impact runoff generation and flow processes by altering the underlying surface and local water usage within the basin. The Loess Plateau, characterized by severe soil erosion and fragile ecosystems, has long been recognized as a unique geological and geomorphological region worldwide. However, since 1999, the government has implemented large-scale afforestation and grassland restoration projects in most areas of northern Shaanxi Province. Monitoring data from 2001 to 2015 show an overall increase in the

Normalized Difference Vegetation Index (NDVI) in the Loess Plateau region, indicating the effectiveness of these policies in alleviating ecological environmental problems in the region. Nevertheless, monitoring data also indicate significant changes in runoff alongside the notable increase in vegetation coverage. This suggests that vegetation changes are directly or indirectly altering regional hydrological cycles. From a physical mechanism perspective, increased land surface vegetation leads to increased rainfall interception and evapotranspiration, altering the original infiltration and groundwater recharge through root water retention, thereby directly influencing the formation and evolution of regional runoff. Therefore, selecting the Hulu River Basin as a case study can explore the effects of climate change and human activities on drought and drought characteristic variables based on the physical mechanisms of regional hydrological cycles. This study can provide references for drought detection and assessment in the Loess Plateau and other climatically similar regions.

2.2 Data description

In order to comprehensively identify and assess drought events in a changing environment, this study utilizes five main types of data: observed runoff data, meteorological data, geographical information data, large-scale climate patterns data and remote sensing datasets related to anthropogenic influences. Daily runoff data were collected from the Yellow River Conservancy Commission covering the period of 1965–2014 at Qin'an station. Daily meteorological data were collected from the China Meteorological Data Sharing Service System, including precipitation, maximum temperature, minimum temperature, solar radiation, mean relative humidity, and mean wind speed covering the period of 1965–2014 at 8 rain gauges. The location of the rain gauges is distributed in Figure 1d. Daily baseflow (*BF*) was calculated using the Chapman-Maxwell filter method. In this study, baseflow (*BF*) is considered as groundwater, as detailed in Supporting Information S1. Daily soil moisture data is simulated by The Soil and Water Asses sment Tool (SWAT) model. The SWAT model for the Hulu River Basin needs spatial data and climate input. The Chinese Academy of Sciences provided a 30-m resolution digital elevation model (DEM) and a digital soil map (1:100,000). According to the Genetic Soil Classification of China, five soil types were identified for the basin. The soil properties of each type were derived from the Chinese Soil Database of the Institute of Soil Science. A 1970s land use map with a resolution of 30×30 m provided by the Chinese Academy of Sciences was used in this study. Materials related to SWAT model simulation results can be found in the Supporting Information S2.

Moreover, six large-scale climate patterns are utilized as external covariates for the nonstationary modelling of precipitation, soil moisture, runoff, and groundwater. They are the Atlantic Multidecadal Oscillation (AMO), the Arctic Oscillation (AO), the North Atlantic Oscillation (NAO), the North Pacific (NP), the Pacific Decadal Oscillation (PDO), and the El Niño/Southern Oscillation (ENSO). This paper measures the inter-annual ENSO state by Southern Oscillation Index (SOI). The monthly time series of these climate patterns were collected from the Climate Prediction Center of NOAA Earth System Research Laboratory (http://www.cpc.ncep.noaa.gov/data/).

The Global Inventory Modelling and Mapping Studies (GIMMS) NDVI3g dataset (https://ecocast.arc.nasa.gov/data/pub/gimms/3g.v1/) was used to analyse vegetation cover dynamics from 1982 to 2014 with a spatial resolution of 1/12°. The Impervious Surface Ratio (ISR) data from 1985 to 2019 at a spatial resolution of 30 m were collected to infer the rate of urbanization (Gong et al., 2020). The ISR dataset was extracted and calculated from the Google Earth Engine platform. Population data (POP) from 2000 to 2019 was obtained from WorldPop (Worldpop, 2018), which is the data on population distributions and dynamics at the high spatial resolution, which characterizes population growth and rural-urban migration. The POP dataset was processed by an unconstrained top-down modelling method into a resolution of 30 arc seconds. Due to the insufficient length of the NDVI, ISR, and POP sequences, a Long Short-Term Memory (LSTM) network was employed to perform nonlinear interpolation on them for the period of 1965-2014.

3 Methods

The objective of this study is to develop a framework for drought monitoring and assessment from a drought propagation perspective under non-stationary environments. There are five steps to achieving this purpose: (1) conducting linear and nonlinear correlation analyses between the 12-month Standardized Precipitation Index (SPI) and the Standardized Soil Moisture Index (SSI), Standardized Runoff Index (SRI), and Standardized Groundwater Index (SGI) at various time lags to explore the patterns of drought propagation; (2) determining the significant climatic and anthropogenic indices via linear and nonlinear correlation analysis to present the large-scale climate anomalies and anthropogenic influence variation; (3) constructing the nonstationary probability model for precipitation, soil moisture, runoff, and groundwater used the climatic and human-induced factors as explanatory variables; (4) computing the NIDI to depict the horary dependence structure for precipitation, soil moisture, runoff, and groundwater by the time-varying copula model; (5) utilizing the NIDI to monitor and assess the droughts and analyse the drought characters. As a case study, the Hulu River Basin in western China was chosen to validate the applicability and effectiveness of the NIDI. The NIDI incorporates precipitation, soil moisture, runoff, and groundwater, climate variation, and anthropogenic activity to assess drought conditions in a changing environment comprehensively. Figure 2 shows the integrated framework for monitoring and assessing drought events from a drought propagation perspective under non-stationary environments. A brief description of the methodology is offered in the subsections below.

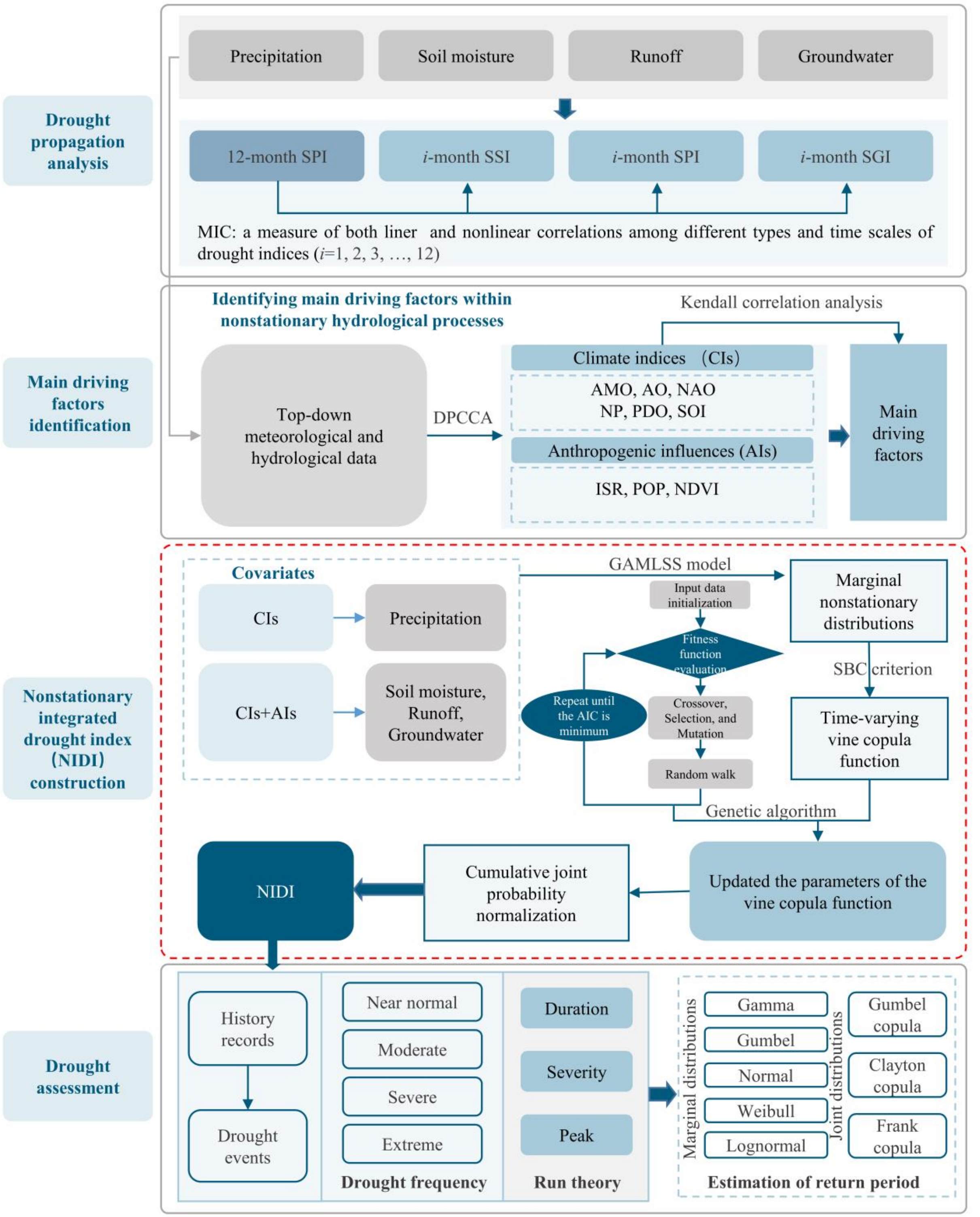

Figure 2. The integrated framework for monitoring and assessing drought events from a drought propagation perspective under non-stationary environments.

3.1 Drought propagation analysis

The propagation of drought is closely tied to fluctuations in the anomalies of hydro-meteorological signals as it moves through interconnected terrestrial components of the hydrological cycle (Heudorfer and Stahl, 2017; Van Loon et al., 2015). Throughout these processes, properties like the timing of different drought stages (e.g., onset, recovery), frequency, duration, severity, and intensity of various drought types may undergo alterations. Various characteristics or features of drought propagation can be established to illustrate the propagation process. These characteristics include, but are not limited to, the response time scale and lag time. Choosing a suitable timescale for the drought index is crucial since drought results from the accumulated impacts of water deficits over disparate periods (F. Wang et al., 2020). In China, precipitation has a pronounced seasonal pattern, the whole annual rainfall transpires within the four monsoon months, namely June to September (Mishra et al., 2012; Rana et al., 2015). Hence, in order to accommodate the seasonal variation in precipitation, we incorporate a 12-month SPI, which represents the total precipitation over a 12-month period, to construct the NIDI. Then, we determined the different timescale for other drought indices by using linear and nonlinear correlation analyses between the 12-month SPI and the SSI, SRI, and SGI at various time lags from the drought propagation perspective.

3.2 Determination of Climate indices (CIs) and Anthropogenic influences (AIs)

Climate indices (CIs):

Six large-scale low-frequency climate indices (AMO, AO, NAO, NP, PDO, and SOI) have been chosen to represent climate indices. A moving average approach is used to smooth the climate indices to reduce the influence of a noisy environment. Based on the results of drought propagation analysis, sliding window averaging is applied to the CIs at different temporal scales according to various drought indices. Meanwhile, the time series for precipitation, soil moisture, runoff, and groundwater are also created by different timescales moving average method. This way, the different monthly fluctuations of precipitation, soil moisture, runoff, and groundwater can be easily discerned and understood. For the correlation studies, the simultaneous time series and the recreated time series with lead times are prepared for precipitation, soil moisture, runoff, and groundwater series in a given month. Kendall's correlation test (Bolboacă and Jäntschi, 2006) was employed to determine the significant precipitation, soil moisture, runoff, and groundwater climatic factors in nonstationary modelling.

Anthropogenic influences (AIs) :

The effects of vegetation dynamics on the hydrological cycle refer to the influence of vegetation growth, coverage, and changes on the movement and distribution of water within an ecosystem (Yu et al., 2023). Vegetation serves as a regulator of land-atmosphere interactions and plays a crucial role in coupling the carbon-water cycles and surface energy balance within the soil-plant-atmosphere system (Claussen et al., 2013). Vegetation interacts with the hydrological cycle through processes such as evapotranspiration, interception, infiltration, and groundwater recharge (Ajami et al., 2017). Conversely, changes in precipitation patterns, rising temperatures, and variations in water availability directly impact vegetation growth and transpiration. In recent decades, afforestation programs have been proposed to harness benefits related to flood mitigation and carbon storage. The impact of afforestation on streamflow across diverse catchments is found to consistently decrease median and low streamflow (Buechel et al., 2022). Consequently, the investigation of vegetation dynamics is underscored as a candidate driving factor in exploring the changes of drought.

The intensification of anthropogenic activities, accompanied by urbanization processes such as population growth, economic development, infrastructure development, and rural-urban migration, has emerged as a global threat to the sustainability of water resources (Mekonnen and Hoekstra, 2016).

However, obtaining long-term and continuous data sequences of anthropogenic activities that are linked to the hydrological cycle presents a significant challenge. Also, acquiring human activity data at the catchment level is difficult. Most associated statistical information is divided based on administrative units such as urban areas, irregular regions, or spanning multiple catchments (Thorslund and Van Vliet, 2020). Remote sensing observations offer powerful tools for analysing and monitoring the impact of human activities on river systems globally. These observations provide extensive datasets that allow for the identification of human pressures and the assessment of their temporal progression and wide spatial distribution (Ceola et al., 2019).

3.3 Construction of the Nonstationary Integrated Drought Index (NIDI)

Investigating the candidate driving factors for changes in precipitation, soil moisture, runoff, and groundwater in non-stationary processes, we consider climate forcing, and anthropogenic influences. Following this, nonstationary probability models are constructed for precipitation, soil moisture, runoff, and groundwater, utilizing both climatic and human-induced factors as explanatory variables. The next step involves computing the NIDI to depict the temporal dependence structure for precipitation, soil moisture, runoff, and groundwater using a vine copula model. Finally, the NIDI is utilized to monitor and assess droughts, as well as analyse their characteristics. The specific calculation steps for NIDI are as follows:

Step 1: Nonstationary marginal distribution modelling

Rigby and Stasinopoulos (2005) proposed the GAMLSS model to construct the connection between the covariates and distribution parameters. This approach is currently extensively employed in nonstationary modelling for hydro-meteorological variables (Gao et al., 2018). In this framework, the probability density function $f_X(x_t | \mu_X^t)$ includes the linkages of time-varying parameters with explanatory variables. This study describes the location parameter as a linear function of the explanatory variables in Eq. (1):

$$\mu_t = a_0 + a_1 I_t^1 + a_2 I_t^2 + \cdots + a_n I_t^n \tag{1}$$

where μ_t denotes the dynamic location parameter; I_t^n presents the nth explanatory variable, and a_i is the coefficient value for each covariate. In addition, the scale parameter also adhered to the same presumption.

Applicable explanatory variables are vital in uncovering the variation of hydrologic elements and nonstationary simulations' success. In this study, the CIs and AIs in Section **Error! Reference source not found.** are assumed to be potential covariates for hydro-meteorological variables modelling. The potential effects of covariates were then explained using three nonstationary models. The nonstationary behaviours may cause by the application of differing statistical parameters, and shown in Table 1. As shown in Table 1, Model 0 presents a stationary model whose two parameters are kept steady. Nevertheless, one or two parameters in the other models fluctuated with variables. In this work, it is essential to note that all nonstationary model parameters and covariates are related to this work via a linear relationship. In general, when the length of the hydro logical sequence is greater than 8, the Schwarz Bayesian Criterion (SBC) criterion is more accurate than the AIC (Zhang, et al. 2021). Hence, the SBC is employed to evaluate the performance of each model. Meanwhile, the worm diagram is used to assist the validation from the perspective of qualitative evaluation.

Table 1. Classification of four models.

Model	Description	μ	σ
0	Stationary	~1	~1
1	Nonstationary	~1	~ covariate
2	Nonstationary	~covariate	~1
3	Nonstationary	~ covariate	~covariate

Step2: Nonstationary joint distribution modelling

There are many pair-copula constructions that can be used for high-dimensional distributions. In order to facilitate organizing, Bedford and Cooke, (2002) devised a graphical paradigm known as the regular vine. A wide range of pair-copula decompositions are encompassed under the class of regular vines. Within this framework, our attention is directed towards the D-vine (Aas et al., 2009) . Based on the non-stationary marginal distribution results obtained from the first step for precipitation, runoff, soil moisture, and groundwater, the D-vine copula function is selected to describe their dependence structure. The general expression for the four-dimensional D-vine structure is:

$$
\begin{aligned}
f(x_1,x_2,x_3,x_4) = {} & f_1(x_1)\cdot f_2(x_2)\cdot f_3(x_3)\cdot f_4(x_4) \\
& \cdot c_{12}\left\{F_1(x_1),F_2(x_2)\right\}\cdot c_{23}\left\{F_2(x_2),F_3(x_3)\right\}\cdot c_{34}\left\{F_3(x_3),F_4(x_4)\right\} \\
& \cdot c_{13|2}\left\{F(x_1|x_2),F(x_3|x_2)\right\}\cdot c_{24|3}\left\{F(x_2|x_3),F(x_4|x_3)\right\} \\
& \cdot c_{14|23}\left\{F(x_1|x_2,x_3),F(x_4|x_2,x_3)\right\}
\end{aligned}
\tag{2}
$$

where $f(\cdot)$ presents the marginal distribution, $c(\cdot)$ is the copula function at different edge.

The D-vine copula function that includes significant CIs and AIs as covariates can describe the horary dependence structure between different hydro-meteorological variables in a varying environment. A linear relationship between the copula parameters and the covariates is described as follows:

$$\theta_C^t = b_0 + b_1 I_t^1 + b_2 I_t^2 + \cdots + b_n I_t^n \tag{3}$$

where b_i presents the coefficient value for each covariate, θ_C^t represents the dynamic parameter of time-varying copulas.

Then the nonstationary joint distribution is computed as follows:

$$P(X^t,Y^t,U^t,V^t)=C\left[F_X(x_t|\theta_X^t),F_Y(y_t|\theta_Y^t)\middle|\theta_C^t,F_U(u_t|\theta_X^t),F_V(v_t|\theta_X^t)\right]=C(x^t,y^t|u^t,v^t|\theta^t) \tag{4}$$

$$NIDI=\varphi^{-1}\left[P(X^t,Y^t,U^t,V^t)\right] \tag{5}$$

where x, y, u, v are precipitation, soil moisture, runoff, and groundwater, respectively; the θ_X^t, θ_Y^t, θ_U^t and θ_V^t are the dynamic parameters of the marginal distributions; $P(X^t,Y^t,U^t,V^t)$ presents the cumulative distribution probability of nonstationary joint distribution; $\varphi^{-1}(\cdot)$ presents the standard normal distribution. The copula functions' parameters at different edge are computed by the maximum likelihood estimation. In addition, the optimal distribution will be determined from a comparison with Gaussian, Student t, Clayton, Gumbel, Frank, and Joe copula functions via the Akaike information criterion (AIC) (Akaike, 1973).

Step3: Vine copula's parameters estimation and update

Nasr and Chebana (2022) proposed a new method for estimating parameters in mixture copula models. They utilized a metaheuristic algorithm in conjunction with maximum pseudo-likelihood. An empirical investigation was carried out to evaluate its efficacy, juxtaposing it with commonly employed established techniques. The findings suggest that the suggested methodology yields more precise parameter estimations, even when dealing with restricted sample sizes, hence outperforming traditional techniques. To enhance the performance of the vine copula and accurately estimate the parameters of each edge's copula function, this study employs the following method to estimate and update the copula function parameters:

Initialization: Begin by initializing the vine copula model with initial parameter estimates.

Genetic Algorithm Parameter Estimation: Utilize a genetic algorithm (GA) to estimate the parameters of the copula functions. GA is a metaheuristic optimization algorithm inspired by the process of natural selection and evolution. It can effectively search for optimal or near-optimal solutions in complex search spaces.

AIC Criterion Evaluation: Evaluate the performance of the vine copula model using the AIC. It balances the goodness of fit of the model with the complexity of the model, penalizing overfitting.

Parameter Update: Update the parameters of the copula functions based on the optimization results obtained from the GA. This update process aims to improve the fit of the vine copula model to the data and optimize its performance.

3.4 Drought assessment

Based on the constructed NIDI, this study will comprehensively evaluate drought events from following aspects.

Drought features identification:

According to computation principles like the SPI, SRI, SSI, and SGI, droughts can be divided into different levels via NIDI. Table 2 shows the different drought grades of the NIDI and. Based on the different drought grades, drought properties can be extracted by run theory (Yevjevich 1967).

Table 2. The threshold values and descriptions of the NIDI in this study.

Description	Values
Extreme drought	<-2.00
Serious drought	-1.50 to -1.99
Moderate drought	-1.00 to -1.49
No drought	>-1.00

In previous studies, the effectiveness of the run theory has been validated (Chang et al., 2016). At present, it is broadly used for recognizing drought events. Due to the convenience and flexibility of the run theory, it already is a classical method for recognizing drought features (Wu et al., 2020). Therefore, this work used the run theory to identify the features of drought events. According to the run theory, the drought event began with an index value was less than −1. It precluded if the drought index value was more significant than −1.5 and lasted just one month. Additionally, this work will combine two drought events if they with an interval of just one month. Meanwhile, the drought duration of these two drought events will be the sum of them.

Bivariate frequency analysis:

Bivariate frequency analysis is performed using the retrieved drought characteristic variables. Following the steps of the copula function model construction, initially, the Gamma, Gumbel, Normal, Weibull, and Lognormal functions are utilized for marginal distribution fitting and optimization. Subsequently, the Clayton, Gumbel, and Frank functions are employed for fitting and optimization. After obtaining the joint distribution of drought characteristic variables, the return period in two cases was analyzed, including "and" and "or", and the equations are listed as follows:

$$P_{and}(D > d \cap S > s) = 1 - \left[F_D(d) - F_S(s) + C^{\theta}(F_D(d), F_S(s)) \right] \tag{6}$$

$$T_{and} = \frac{E(l)}{P_{and}(D > d \cap S > s)} \tag{7}$$

$$P_{or}(D > d \cup S > s) = 1 - C^{\theta}(F_D(d), F_S(s)) \quad (8)$$

$$T_{or} = \frac{E(l)}{P_{or}(D > d \cup S > s)} \quad (9)$$

where, the return period for the "and" and "or" scenarios is denoted as T_{and} and T_{or}, respectively. The expectation of the drought interval is represented as $E(L)$. $F_D(d)$ and $F_S(s)$ are the marginal cumulative distribution probabilities of drought duration and severity, respectively; $C^{\theta}(F_D(d), F_S(s))$ *)* is the joint cumulative distribution probability of drought duration and severity.

4 Results

4.1 Drought propagation analysis

Before conducting drought propagation analysis, linear regression analysis is used between precipitation and soil moisture, runoff, and groundwater, as shown in Figure 3a, 3b, 3c. The correlation between precipitation and soil moisture and runoff is higher than that with groundwater. When conducting drought propagation analysis, it's crucial to consider the lag time. This temporal delay between various periods or stages (such as onset, persistence, recovery) of meteorological drought and other types of drought is commonly utilized to characterize drought propagation. We determined the different timescale for other drought indices by using linear and nonlinear correlation analyses between the 12-month SPI and the SSI, SRI, and SGI at various time lags. Figure 3d, 3e, 3f shows the Mutual Information Coefficient (MIC) (as detailed in Supporting Information S3) results for the 12-month SPI and *i*-month SSI, SRI, SGI. From Figure 3d, 3e, 3f, we can observe that the propagation time from meteorological drought to agricultural drought is 1 month, to hydrological drought is 4 months, and to groundwater drought is 6 months. The occurrence of such results is highly likely due to the characteristics of the Loess Plateau region, where soil water retention capacity is weak, and groundwater is buried deeply. Consequently, the propagation of meteorological drought to hydrological drought and groundwater drought in this region requires a certain amount of time. Therefore, the 1-month SSI, 4-month SRI, and 6-month SGI are selected to construct NIDI.

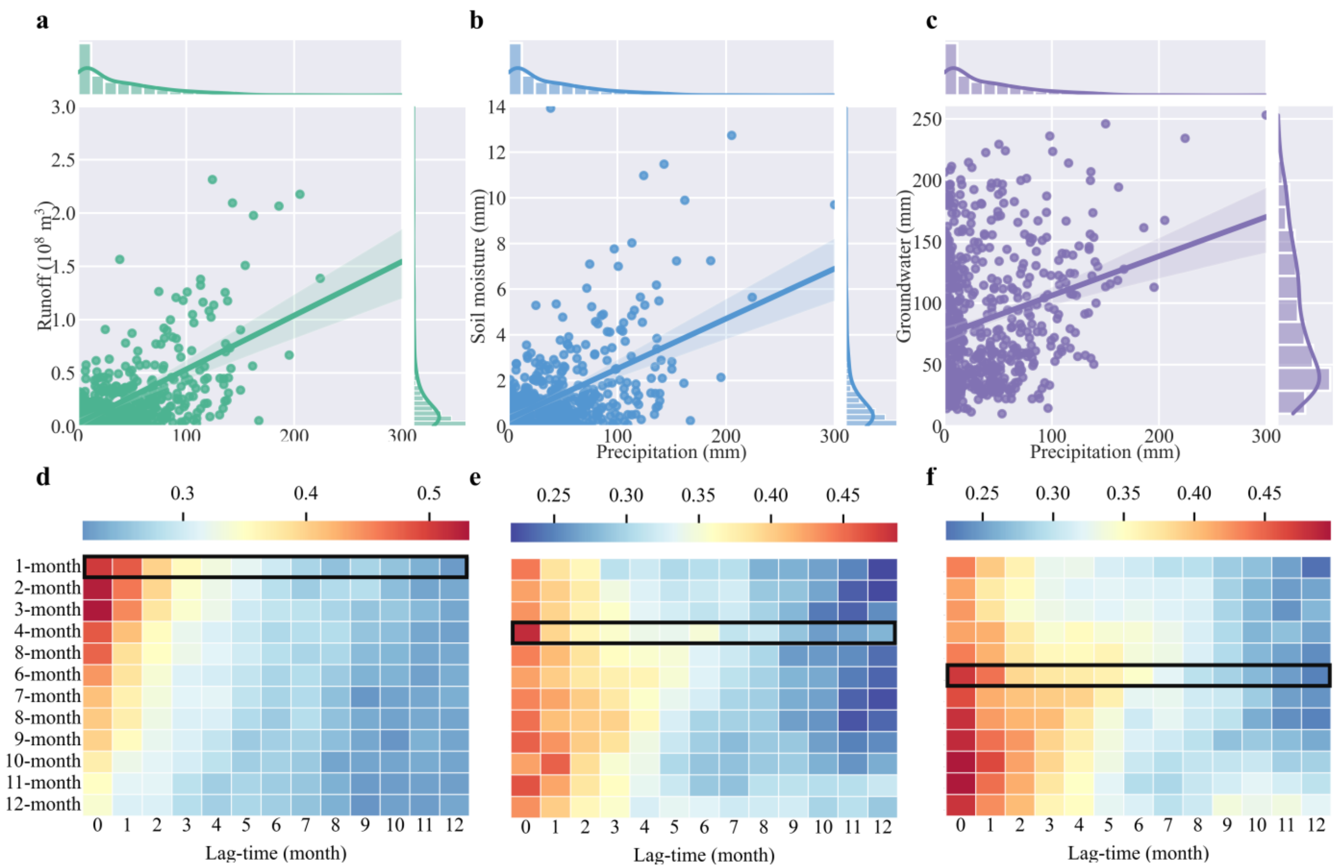

Figure 3. The linear fit between precipitation and **a,** soil moisture; **b,** runoff; **c,** and groundwater. **d,** The Mutual Information Coefficient (MIC) results plot for the 12-month SPI and *i*-month SSI; e, the 12-month SPI and *i*-month SRI; **f,** the 12-month SPI and *i*-month SGI at various time lags.

4.2 Calculation of the explanatory variables

The climatic influencing factors and human activities influencing factors selected in this study are illustrated in Figure 4. Figure 4a displays different atmospheric circulation indices. Figure 4b shows the NDVI for the years 1982, 1998, and 2014. Figure 4c illustrates the ISR for the years 1985, 1999, and 2014. Figure 4d depicts the variations in POP for the years 2000, 2007, and 2014. Figure 4e represents the Pearson correlation analysis results among these influencing factors, while Figure 4f illustrates the MIC results among these influencing factors. As shown in Figure 4, the correlation among climate impact factors is stronger than the correlation between climate factors and human activity factors. Additionally, the correlation among human activity impact factors is stronger than the correlation among climate impact factors. Figure 5a presents the results of the Detrended Partial-Cross-Correlation Analysis (DPCCA) (Yuan et al., 2015, as detailed in Supporting Information S4) between precipitation and climate indices and anthropogenic influences. Figure 5b, 5c, 5d presents the results of dpcca between soil moisture, runoff, and groundwater and climate indices and anthropogenic influences, respectively. From the figure, it is evident that there are varying distributions of dpcca values between different influencing factors and hydro-meteorological variables. Some distributions fall within [-1.0,0.5], while others fall within [-0.2,1.0]. This variability can be attributed to the susceptibility of hydro-meteorological variables to seasonal influences, whereby responses to different influencing factors vary across different years and seasons.

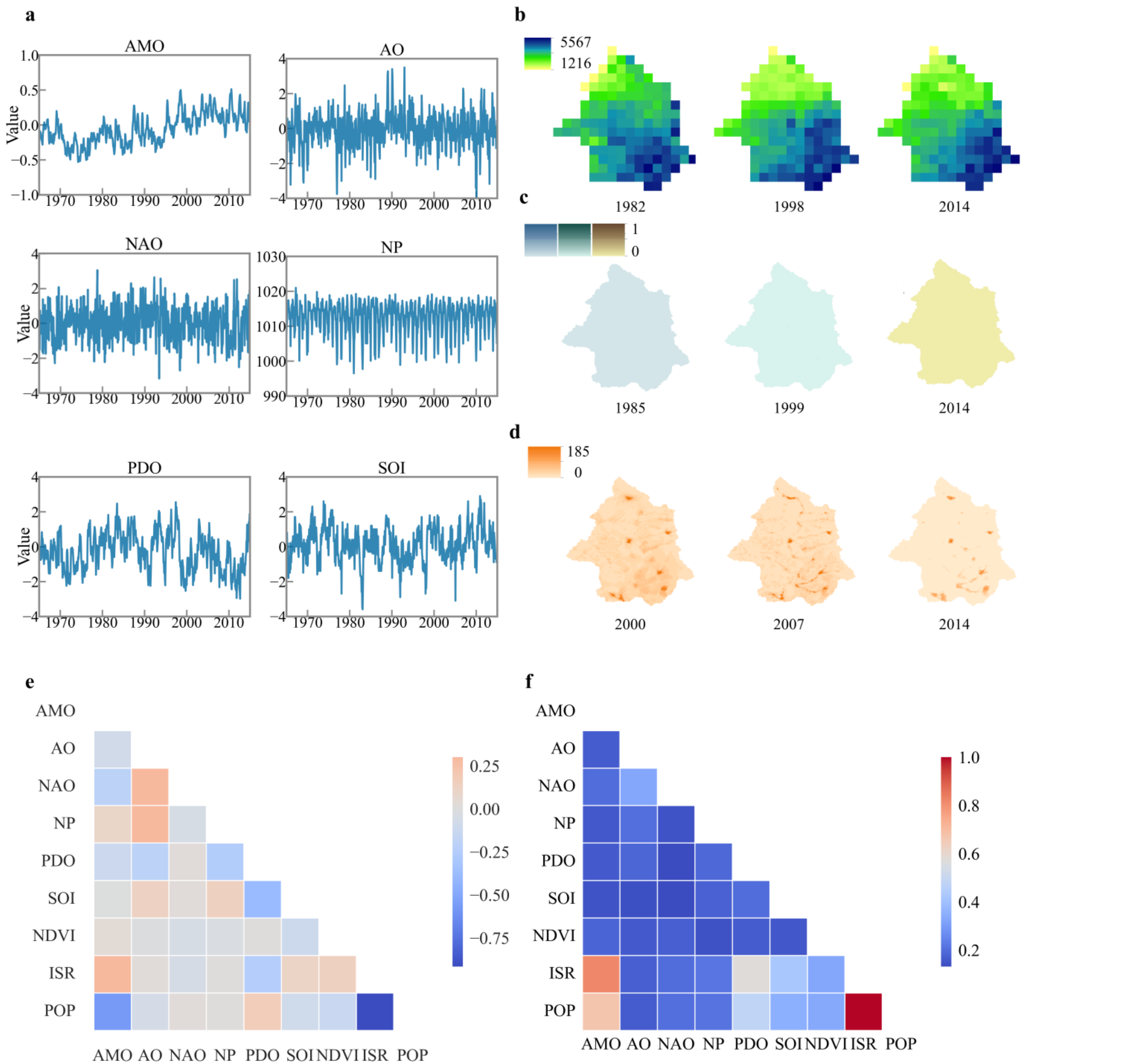

Figure 4. a, The plot of large-scale climate circulation indices. The map of **b,** the Normalized Difference Vegetation Index (NDVI), **c,** the Impervious Surface Ratio (ISR), and **d,** Population (POP). **e,** The results of Pearson correlation analysis between climate indices and anthropogenic influences. **f,** The MIC results between climate indices and anthropogenic influences.

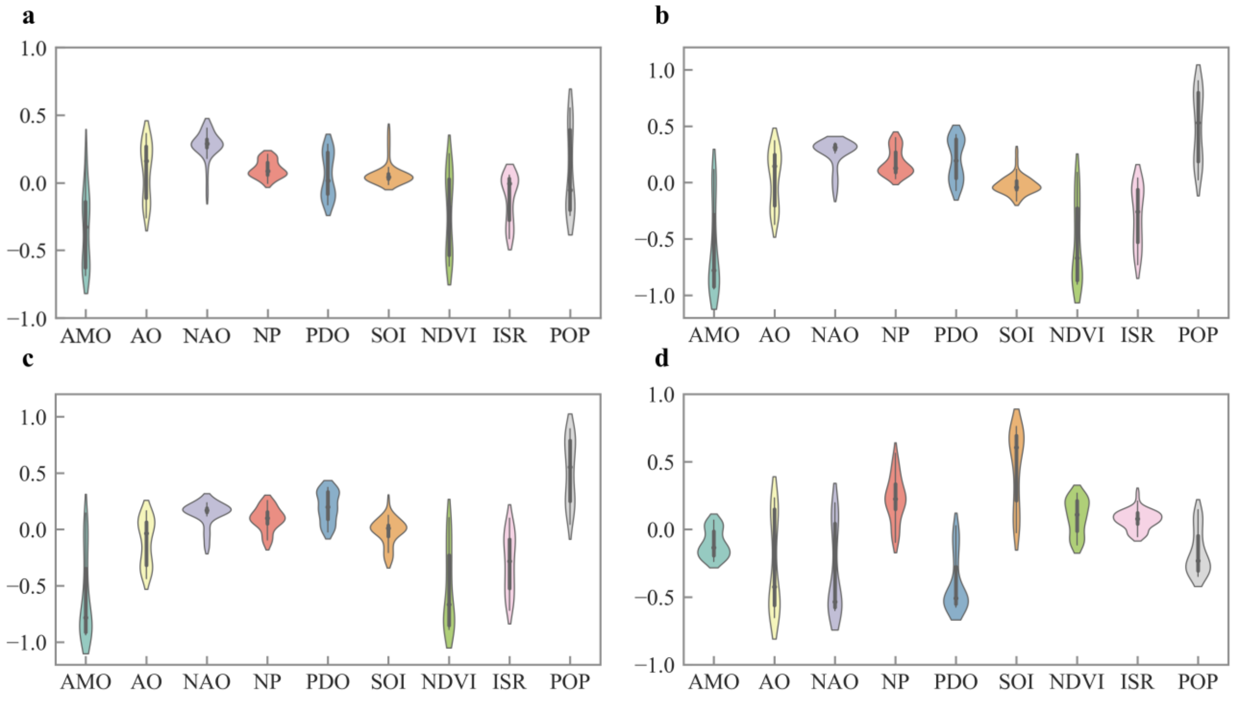

Figure 5. The results of dpcca between **a,** precipitation **b,** soil moisture, **c,** runoff, **d,** and groundwater and climate indices and anthropogenic influences, respectively.

The influence of large-scale climate circulation patterns on hydro-meteorological variables is not instantaneous; it exhibits time lag. In other words, changes in hydro-meteorological variables may occur after a certain period following the occurrence of atmospheric circulation patterns. In order to consider the influence of different large-scale climate circulation patterns at various time lags on different hydro-meteorological variables, Kendall correlation tests were conducted on them. The results are depicted in Figure 6. As shown in Figure 6, precipitation in most months had significant correlations with the SOI. Similarly, the AMO had a strong connection with runoff and soil moisture, and groundwater has a significant connection with PDO. Moreover, hydro-meteorological variables at different months were highly correlated with distinct climate patterns and the leading times. For example, the precipitation in May presented a significant connection to the 1-month leading AMO, 12-month leading NAO, 4-month leading NP and 7-month leading SOI. In March, the precipitation notably correlated with the AMO in last November, NP in last October and the SOI in last July. Besides, the soil moisture in October dramatically connected with the AMO and NP in September, and the PDO in March. The February runoff remarkably correlated with the AMO in last July, NAO in last December and SOI in last August. In May, the groundwater strongly correlated with the NP and SOI in March, PDO in last October. It implies that the climate indices correlate with precipitation, soil moisture, runoff, and groundwater highly, which may induce their variation.

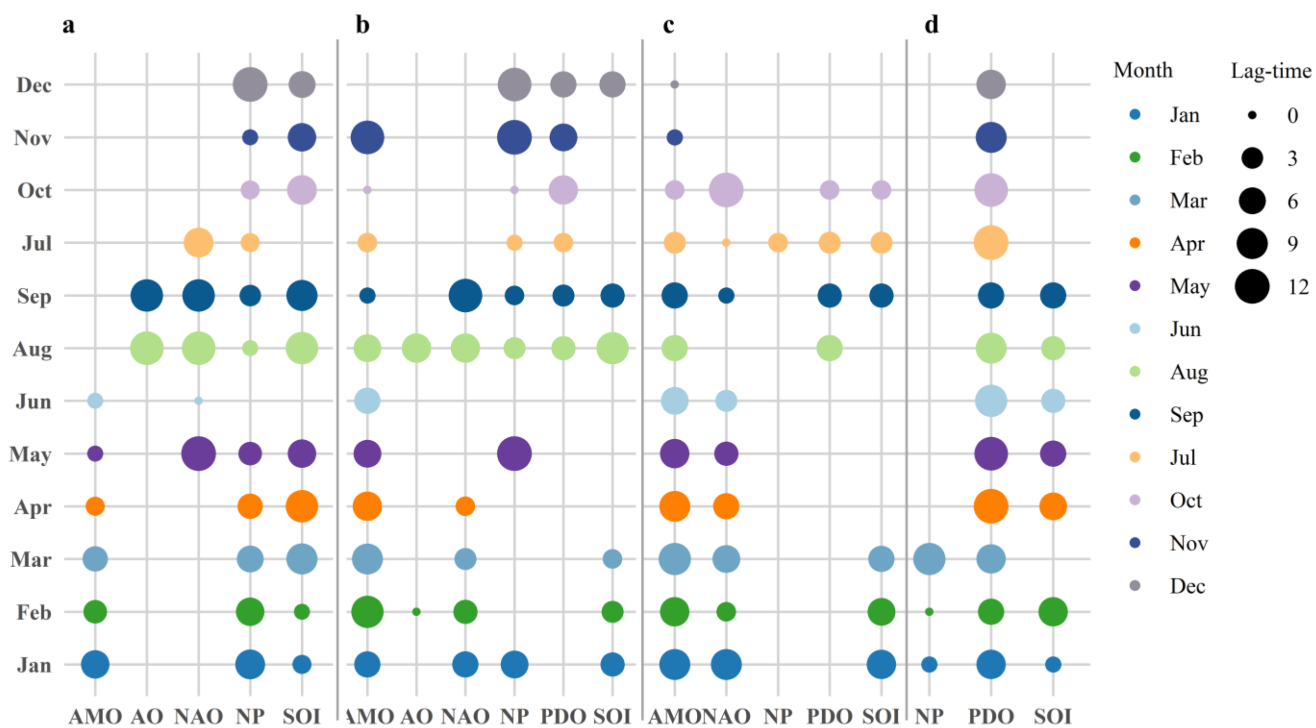

Figure 6. The results of Kendall correlation analysis between **a,** precipitation, **b,** soil moisture, **c,** runoff, **d,** and groundwater and different 5 lag-time climate indices, respectively.

4.3 Modelling with the nonstationary marginal and joint distributions

The assumption of stationarity for hydro-meteorological variables is no longer valid due to the impact of climate change and human activities. Consequently, stationary probability models have challenges in accurately representing the dynamic trends and evolutionary patterns of these variables. Therefore, this study adopts non-stationary probability models to fit hydro-meteorological variables, aiming to reveal their response to climate change factors and human activity factors. For this purpose, five widely used distributions (Gamma, Gumbel Normal, Weibull and Lognormal) were employed for the candidates in this work. Then, they were utilized to fit the 12-month scale precipitation, 1-month scale soil moisture, 4-month scale runoff, and 6-month scale groundwater series. The CIs were used as explanatory variables to construct the nonstationary marginal distributions of precipitation in different months. Similar to precipitation, soil moisture, runoff, and groundwater will establish the nonstationary marginal distributions for different months using CIs and AIs. The SBC criterion was used for the goodness of fit (GOF) test, and the results are shown in Figure 7. The optimal distribution functions for precipitation, soil moisture, runoff, and groundwater varied between the months in Figure 7. As shown in Figure 7a, the Normal distribution displayed the best fit (smallest GOF values) with precipitation in July, October November and September, while other distributions fit better with precipitation in the rest of the months. Like precipitation, different distributions presented the best fit for soil moisture, runoff, and groundwater data during the various months (shown in Figure 7b,7c,7d). The Gamma and Lognormal distributions were the optimal options in most months.

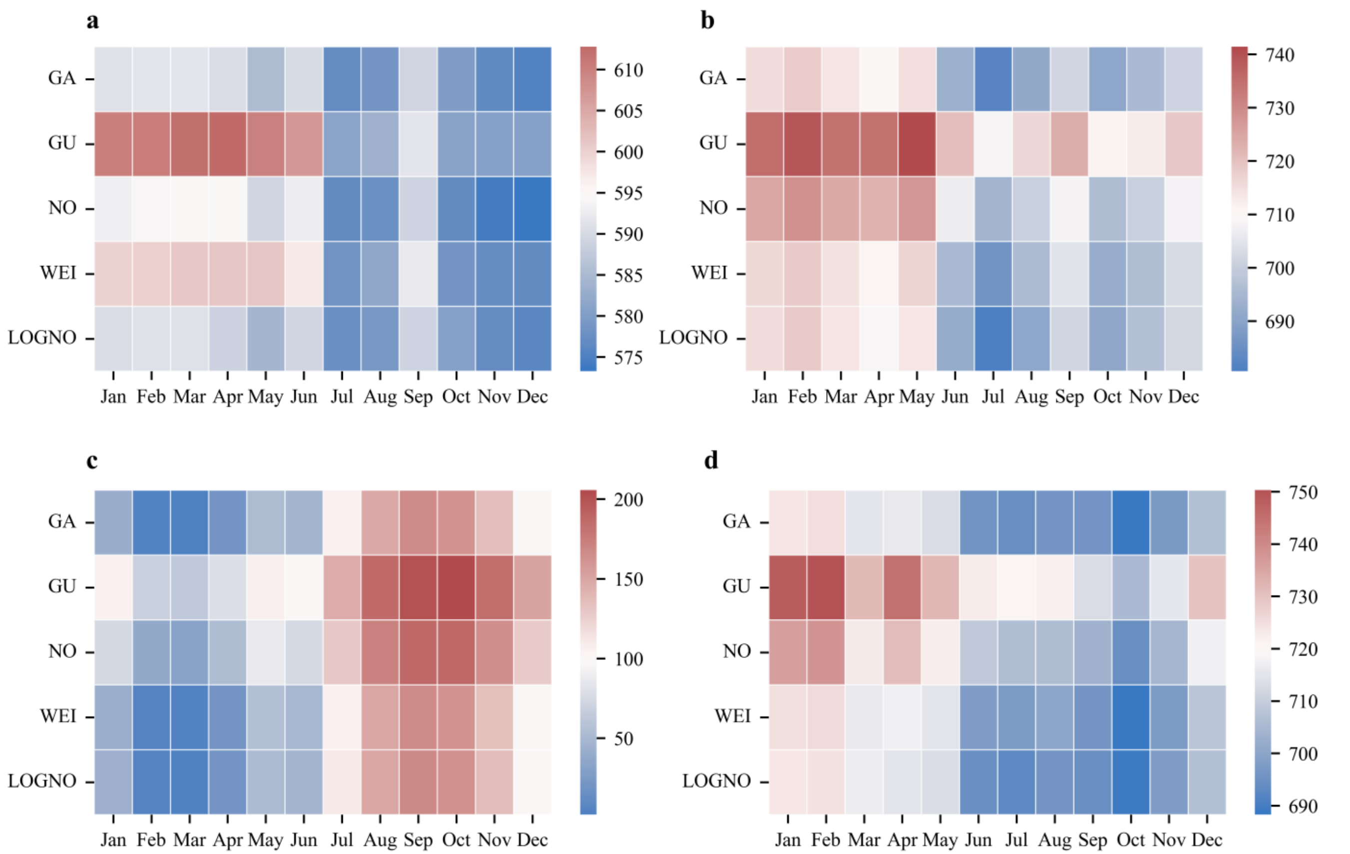

Figure 7. The SBC results of nonstationary marginal distributions for **a,** precipitation, **b,** soil moisture, **c,** runoff, and **d,** groundwater, respectively.

Based on the non-stationary marginal distribution models of the hydro-meteorological variables described above, a D-vine copula function was utilized to capture their dependence, as illustrated in the Table 3. The Table 3 provides information on the structure of the vine copula, as well as the copula functions and their parameters at different edges. By comparing the AIC values obtained from different parameter estimation methods, it can be observed that, in comparison to conventional maximum likelihood estimation, the GA can more accurately estimate the parameters of copula functions, thus enhancing the performance of the vine copula function. Therefore, we utilize the parameters estimated by the GA to update the vine copula function, preparing for the subsequent construction of the NIDI.

Table 3. Results of the time-varying vine copula function.

tree	edge	copula	MLE		GA	
			par	AIC	par	AIC
1	3,2	Gumbel copula	3.1969	-881.14	3.1938	**-881.88**
	1,3	Normal copula	0.5142	-171.63	0.5147	**-171.93**
	4,1	Normal copula	0.6582	-331.21	0.6583	**-331.30**
2	1,2;3	Frank copula	0.3350	0.16	0.3415	**0.18**
	4,3;1	Normal copula	0.1306	-7.67	0.1354	**-7.85**
3	4,2;1,3	Joe copula	-0.6320	-14.42	-0.6215	**-14.89**

4.4 Construction and validation of the NIDI

Building upon the foundation of non-stationary marginal distributions, we employed time-varying vine copula functions to construct NIDI. Furthermore, we utilized genetic algorithms for parameter estimation and updating of the constructed NIDI. Based on the proven applicability of the SPI, SRI, SSI, and SGI, the NIDI was evaluated by comparing its reliability to these indices. According to Figure 8a, 8b, and 8c, similar variations are observed in SPI, SRI, SSI, SGI, and NIDI in general, implying that NIDI can determine drought conditions effectively. the correlation between NIDI and SPI, SSI, and SRI is relatively strong, while its correlation with SGI is weaker. Moreover, the NIDI is able to characterize both hydrological and meteorological drought simultaneously, which is an advantage of a comprehensive drought index. In general, both the SPI, SRI, SSI, SGI, and NIDI had similar temporal trends, and they both performed well during droughts. From Figure 8e, 8f, and 8g, it can be observed that the drought duration distribution extracted by NIDI is relatively uniform without significant outliers. The severity of drought extracted is strong and comparable to SPI. However, the peak drought values extracted are the most extreme, indicating that NIDI can identify more extreme drought situations compared to SPI, SRI, SSI, and SGI.

Due to the lack of historical drought information for the Hulu River basin, the historical records for the Wei River basin will be adopted as references in this study. The historical records (Wen and Ding, 2008) in the Wei River basin, indicate periods of typical drought events to be October 1979 to May 1980, January 1995 to May 1996, April 1997 to March 1998, November 1998 to April 1999, March 2001 to August 2001, and May 2008 to August 2008. Comparing these drought events showed that the droughts recognized by NIDI were in line with history, further verifying the dependability of the NIDI. However, there are some notable differences, particularly in results prior to 1992. According to Figure 8, the NIDI was lower than the SPI, SRI, SSI, and SGI prior to 1992, indicating the NIDI recognized more extreme drought events in comparison with the them. Moreover, the droughts detected by the NIDI were usually more severe than SPI, SRI, SSI, and SGI in most situations. This difference leads to differing grades between the two drought indexes. For instance, the NIDI recognized a drought event sustained from May 2004 to October 2004, while the SGI did not identify a drought event throughout the same time. In this case, the difference in results between the NIDI and SPI, SRI, SSI, and SGI is due to they taking the stationary model of the entire time series as its basis. As a result, the SPI, SRI, SSI, and SGI typically underrated extremes and had a lower performance at capturing local variability in series. Conversely, the NIDI is calculated using a nonstationary model, composing climatic and human-induced influence information. It implies this model can more precisely compute extreme precipitation, soil moisture, runoff, and groundwater under changing environments.

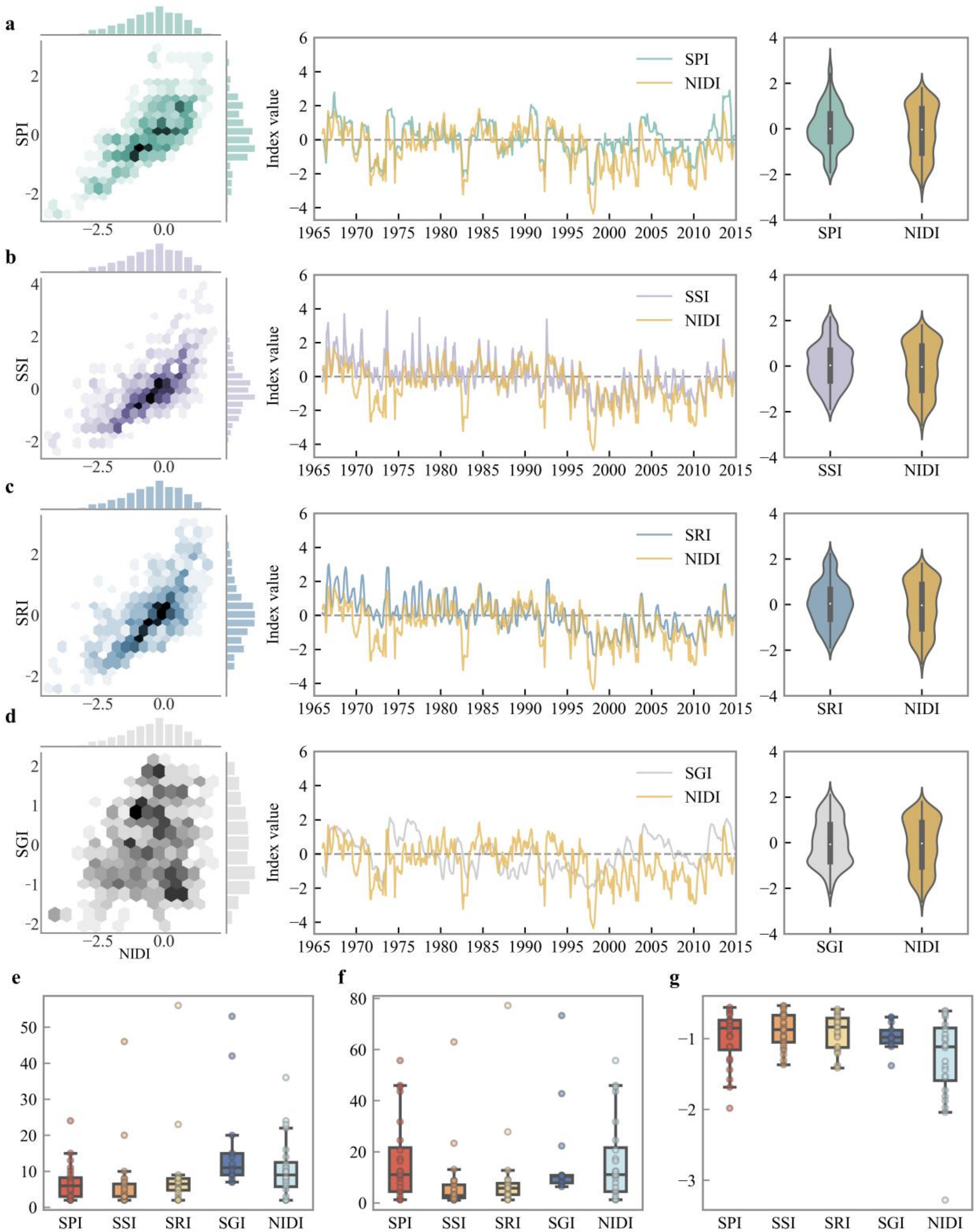

Figure 8. The linear regression plots, trend plots, and violin plots of NIDI with respect to **a,** SPI, **b,** SSI, **c,** SRI, and **d,** SGI, respectively. The comparative plots of **e,** drought duration, **d,** drought severity, and **f,** drought peak extracted from different drought indices.

4.5 Drought frequency analysis

We divided the study period into five parts, namely period A (1966–1975), period B (1976–1985), period C (1986–1995), period D (1996–2005), and period E (2006–2014). We extracted the frequencies of near-normal drought, moderate drought, severe drought, and extreme drought using different drought indices for each period. From Figure 9a, it is evident that all five indices can extract near-normal drought frequencies, but during 1996–2005 and 2006–2014, the frequency of NIDI was lower than the other four indices. In Figure 9b, regarding moderate drought frequencies, the NIDI frequency is lower than the other four indices during 1976–1985 and 1986–1995, but it performs well in other years, even surpassing the other indices during 1966–1975. Moving to the severe drought section, some indices fail to identify severe drought during 1966–1975, 1976–1985, and 1986–1995, but NIDI performs well. However, in the extreme drought section, NIDI exhibits superior performance, identifying extreme drought in all years when other indices fail to do so.

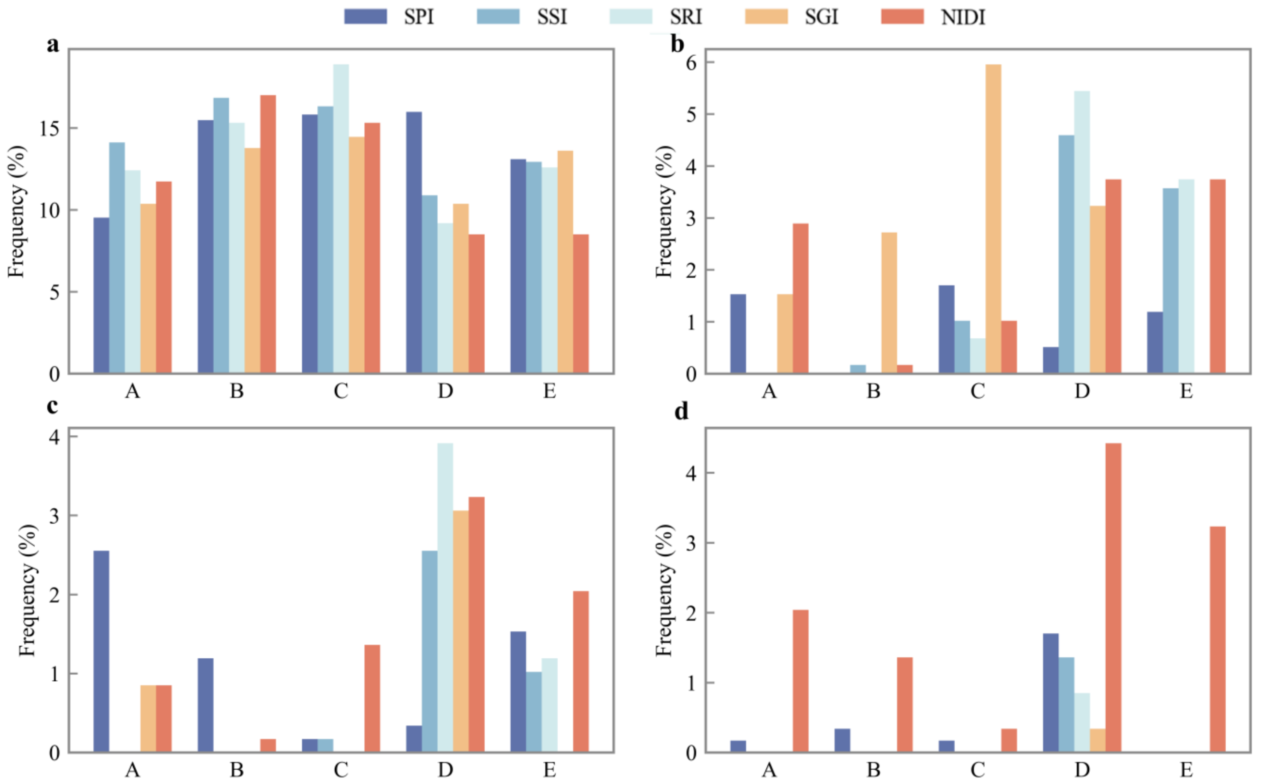

Figure 9. Frequency of **a,** near normal drought, **b,** moderate drought, **c,** severe drought, **d,** extreme drought in different periods identified by the NIDI and SPI, SSI, SRI, SGI in the study area. The hydrological drought indexes sequences were divided into three sections, i.e. period A (1966–1975), period B (1976–1985), period D(1986–1995), period D (1996–2005), period E (2006–2014).

In addition, this study conducted bivariate frequency analysis on drought characteristic variables identified by NIDI. Firstly, marginal distribution fitting was performed on drought duration, severity, and peak values. Five widely used distributions (Gamma, Gumbel, Normal, Weibull, and Lognormal) were considered as candidates in this analysis. Subsequently, joint distribution fitting was carried out using bivariate copula functions. Finally, the recurrence period of drought events under the cases of "and" and "or" was computed. Based on Figure 10a, 10b, and 10c, the corresponding drought characteristic variables for any joint probability could be obtained. Meanwhile, Figure 10d and 10e provides the drought return periods under specified joint probabilities.

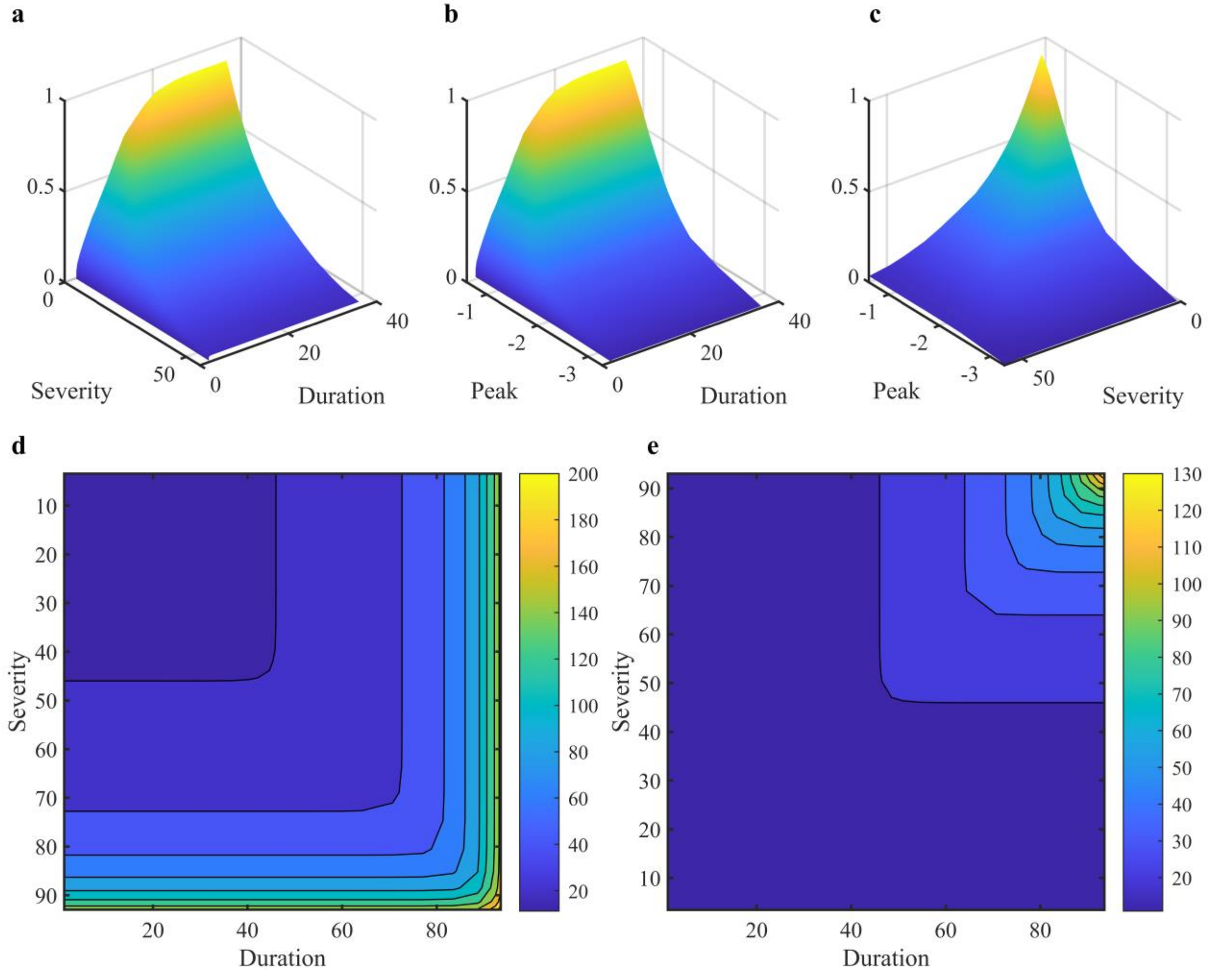

Figure 10. Joint distribution of NIDI's **a,** duration and severity, **b,** duration and peak, **c,** severity and peak. The recurrence period of drought events under the cases "and" and "or" estimated by the NIDI (**d** & **e**) for the study area.

5 Discussion

Drought indices have been widely applied to drought monitoring and drought assessment because of their characteristics that can quantitatively represent drought events. Generally, traditional drought indices are calculated from a sole variable under the assumption of stationary. However, the statistical features of hydro-meteorological variables change with time as climate variation and anthropogenic impacts intensify. Thus, a stationary method would lead to invalid calculations, which would further impact the accuracy of drought monitoring and assessment (Jiang et al., 2019). Moreover, the standardized drought index based on a single hydro-meteorological variable cannot capture drought information comprehensively. Previous studies have pointed out that it was necessary to propose a multivariate drought index that considers climate and anthropic-induced nonstationary (Zhang et al., 2021; Song et al., 2020). This index can obtain the drought characteristics from a comprehensive perspective. Thus, this paper proposed an integrated nonstationary drought index (NIDI) incorporating precipitation, soil moisture, runoff, and groundwater, climate variation, and anthropogenic activity.

The advantage of the NIDI is that it combines the response to meteorological, agricultural, hydrological and groundwater droughts whereas considering climate change and anthropogenic influence. This paper used significant large-scale climatic indices (CIs) as explanatory variables to indicate the climate variation. Additionally, anthropogenic influence (AIs) is assessed using indicators such as the NDVI, ISR, and POP. Meanwhile, the fluctuating behaviour of the soil moisture, runoff, and groundwater series could be represented in the nonstationary modelling by incorporating CIs and AIs as covariates. Therefore, the NIDI proposed in this study could offer a novel perspective to construct comprehensive nonstationary drought indices under a variation environment. Results show that NIDI has effectively identified historical drought events and provided a more comprehensive reference for drought monitoring and assessment.

Previous research has pointed out that the AO and the NAO impact the evolution of drought in Northwest China (Wang et al., 2015). Results showed that precipitation was strongly connected with the NP and SOI, while soil moisture and runoff were closely linked with the AMO, and groundwater was significant connected with PDO in Hulu River Basin (Figure 6). This could be attributed to the location of the Hulu River Basin in the Loess Plateau region, characterized by high terrain, arid climate, weak soil water retention capacity, and deep groundwater burial, resulting in a delayed response to the AO and NAO. Taking large-scale CIs as covariates can reappear the variation of the precipitation, soil moisture, runoff, and groundwater series in nonstationary modelling (Figure 7), producing lower SBC values. In addition to the effect of climate variability on drought, the influence of anthropogenic activities should have a constant and dynamical evolution over time. In the nonstationary modelling for the Hulu river basin, the AIs was always an explanatory variable of the best nonstationary model in 12 months. It suggested the crucial role of anthropic activities in explaining the nonstationary of soil moisture, runoff, and groundwater. As a result, the NIDI has the potential to overcome the limitations of the stationary multivariate standardized drought index and produce more reliable results.

In the case study, the SPI, SRI, SSI, and SGI are chosen for comparative analysis with the NIDI. These three drought indices are chosen as comparative indices because they are calculated with similar data sources as the NIDI, and their applicability has been proved in the previous study. The case study shows that the NIDI has good consistency and is different from the SPI, SRI, SSI, and SGI. However, SPI, SRI, SSI, and SGI are calculated based on only a single hydro-meteorological variable, so they do not comprehensively characterise drought. In this study, the results of the drought assessment indicate that the drought conditions identified by the NIDI are better with the facts than the stationary standard indices. According to NIDI estimates, extreme drought events have occurred frequently in the Hulu River Basin in recent years. The overall difference in results between SPI, SRI, SSI, and SGI and NIDI illustrates that climate change significantly affects hydrological drought conditions in the Hulu River basin. Therefore, an update to the nonstationary drought index is urgently needed to provide more reliable and comprehensive drought information. The proposed NIDI in this study combines the responses of meteorological and hydrological droughts while considering climate change and anthropogenic influence.

Hence, the NIDI is able to consider the nonstationary behaviour of hydro-meteorological variables and can be regarded as an improvement over the traditional drought index under nonstationary conditions.

The NIDI index still has certain limitations that need to be explicitly stated. (1) The soil moisture data were simulated using the SWAT model, which may contain errors compared to actual measurements. Utilizing long-term remote sensing data could potentially provide more accurate results. (2) Due to the lack of future climate influencing factors and human activities, this study did not forecast future drought conditions. However, employing machine learning methods to simulate and predict future influencing factors, combined with downscaled data from CMIP6 General Circulation Models (GCMs), could enable the identification and assessment of future drought conditions. (3) This study only selected three human activity factors, but the influence of human activities on hydro-meteorological variables is complex and diverse. In future research, more representative and comprehensive human activity factors will be chosen to participate in drought studies.

6 Conclusions

The mechanism and propagation process of drought are highly complex. Standardized drought indices constructed based on the assumption of stationarity with single variables are inadequate for accurately identifying and evaluating drought. Therefore, in this study, based on the analysis of drought propagation process, NIDI was constructed using top-down hydro-meteorological variables and propagation time. NIDI also considers the dual impact of climate change and human activities, thus enabling comprehensive identification and analysis of drought characteristics in a changing environment.

A nonstationary model involving climatic and human-induced covariates provides a better fit for hydro-meteorological variables than a stationary model. In the Hulu River basin, the climatic covariates (especially SOI and AMO) may provide insight into non-stationarity in precipitation, soil moisture, runoff, and groundwater. Additionally, the exhibits significant effects on model fitting. It indicates that the introduction of AIs can improve the model's performance to reappear the soil moisture, runoff, and groundwater variation.

A performance comparison between the SPI, SRI, SSI, and SGI showed that the NIDI has a strong statistical correlation with the other three drought indices. In addition, the NIDI can detect and assess droughts directly in a changing environment because it considers the non-stationarities of hydro-meteorological variables. Results revealed that the NIDI recognizes more reliable and acceptable for the Hulu River Basin in historical drought assessments. The NDI could reconstruct the historical drought extremes effectively. Moreover, the NIDI illustrated that the Hulu River Basin had undergone more frequent and severe droughts in recent decades.

According to nonstationary assumptions, drought analysis becomes more challenging. From a comprehensive perspective, this paper provides an innovative approach to monitoring and assessing drought in a changing environment. It can provide valuable references for accurate drought detection and effective drought-related policy-making.

Declaration of Competing Interest

The authors declare that they have no known competing financial interests or personal relationships that could have appeared to influence the work reported in this paper.

Acknowledgments

The work described in this paper was supported financially by the National Natural Science Foundation of China (NSFC) (Grant No. 52179005 and No. 52209006).

References

Aas, K., Czado, C., Frigessi, A., Bakken, H., 2009. Pair-copula constructions of multiple dependence. Insurance: Mathematics and Economics 44, 182–198. https://doi.org/10.1016/j.insmatheco.2007.02.001

AghaKouchak, A., 2014. A baseline probabilistic drought forecasting framework using standardized soil moisture index: application to the 2012 United States drought. Hydrol. Earth Syst. Sci. 18, 2485–2492. https://doi.org/10.5194/hess-18-2485-2014

Ajami, H., Sharma, A., Band, L.E., Evans, J.P., Tuteja, N.K., Amirthanathan, G.E., Bari, M.A., n.d. On the non-stationarity of hydrological response in anthropogenically unaffected catchments: An Australian perspective.

Bazrafshan, J., Hejabi, S., 2018. A Non-Stationary Reconnaissance Drought Index (NRDI) for Drought Monitoring in a Changing Climate. Water Resour Manage 32, 2611–2624. https://doi.org/10.1007/s11269-018-1947-z

Bedford, T., Cooke, R.M., 2002. Vines--a new graphical model for dependent random variables. Ann. Statist. 30. https://doi.org/10.1214/aos/1031689016

Bolboacă, S.-D., Jäntschi, L., 2006. Pearson versus Spearman, Kendall's Tau Correlation Analysis on Structure-Activity Relationships of Biologic Active Compounds.

Buechel, M., Slater, L., Dadson, S., 2022. Hydrological impact of widespread afforestation in Great Britain using a large ensemble of modelled scenarios. Commun Earth Environ 3, 6. https://doi.org/10.1038/s43247-021-00334-0

Ceola, S., Laio, F., Montanari, A., 2019. Global-scale human pressure evolution imprints on sustainability of river systems. Hydrol. Earth Syst. Sci. 23, 3933–3944. https://doi.org/10.5194/hess-23-3933-2019

Chang, J., Li, Y., Wang, Y., Yuan, M., 2016. Copula-based drought risk assessment combined with an integrated index in the Wei River Basin, China. Journal of Hydrology 540, 824–834. https://doi.org/10.1016/j.jhydrol.2016.06.064

Chen, J., Liu, Y., Gitau, M.W., Engel, B.A., Flanagan, D.C., Harbor, J.M., 2019. Evaluation of the effectiveness of green infrastructure on hydrology and water quality in a combined sewer overflow community. Science of The Total Environment 665, 69–79. https://doi.org/10.1016/j.scitotenv.2019.01.416

Claussen, M., Bathiany, S., Brovkin, V., Kleinen, T., 2013. Simulated climate–vegetation interaction in semi-arid regions affected by plant diversity. Nature Geosci 6, 954–958. https://doi.org/10.1038/ngeo1962

Dai, A., 2013. Increasing drought under global warming in observations and models. Nature Clim Change 3, 52–58. https://doi.org/10.1038/nclimate1633

Dracup, J.A., Lee, K.S., Paulson, E.G., 1980. On the definition of droughts. Water Resour. Res. 16, 297–302. https://doi.org/10.1029/WR016i002p00297

Forootan, E., Khaki, M., Schumacher, M., Wulfmeyer, V., Mehrnegar, N., van Dijk, A.I.J.M., Brocca, L., Farzaneh, S., Akinluyi, F., Ramillien, G., Shum, C.K., Awange, J., Mostafaie, A., 2019. Understanding the global hydrological droughts of 2003–2016 and their relationships with teleconnections. Science of The Total Environment 650, 2587–2604. https://doi.org/10.1016/j.scitotenv.2018.09.231

Frazier, A.G., Elison Timm, O., Giambelluca, T.W., Diaz, H.F., 2018. The influence of ENSO, PDO and PNA on secular rainfall variations in Hawai‘i. Clim Dyn 51, 2127–2140. https://doi.org/10.1007/s00382-017-4003-4

Gao, L., Huang, J., Chen, X., Chen, Y., Liu, M., 2018. Contributions of natural climate changes and human activities to the trend of extreme precipitation. Atmospheric Research 205, 60–69. https://doi.org/10.1016/j.atmosres.2018.02.006

Guo, Y., Huang, S., Huang, Q., Leng, G., Fang, W., Wang, L., Wang, H., 2020. Propagation thresholds of meteorological drought for triggering hydrological drought at various levels. Science of The Total Environment 712, 136502. https://doi.org/10.1016/j.scitotenv.2020.136502

Han, H., Hou, J., Huang, M., Li, Z., Xu, K., Zhang, D., Bai, G., Wang, C., 2020. Impact of soil and water conservation measures and precipitation on streamflow in the middle and lower reaches of the Hulu River Basin, China. CATENA 195, 104792. https://doi.org/10.1016/j.catena.2020.104792

Hao, Z., AghaKouchak, A., 2013. Multivariate Standardized Drought Index: A parametric multi-index model. Advances in Water Resources 57, 12–18. https://doi.org/10.1016/j.advwatres.2013.03.009

Heudorfer, B., Stahl, K., 2017. Comparison of different threshold level methods for drought propagation analysis in Germany. Hydrology Research 48, 1311–1326. https://doi.org/10.2166/nh.2016.258

Huang, S., Huang, Q., Leng, G., Liu, S., 2016. A nonparametric multivariate standardized drought index for characterizing socioeconomic drought: A case study in the Heihe River Basin. Journal of Hydrology 542, 875–883. https://doi.org/10.1016/j.jhydrol.2016.09.059

Jehanzaib, M., Shah, S.A., Yoo, J., Kim, T.-W., 2020. Investigating the impacts of climate change and human activities on hydrological drought using non-stationary approaches. Journal of Hydrology 588, 125052. https://doi.org/10.1016/j.jhydrol.2020.125052

Jiang, S., Wang, M., Ren, L., Xu, C., Yuan, F., Liu, Y., Lu, Y., Shen, H., 2019. A framework for quantifying the impacts of climate change and human activities on hydrological drought in a semiarid basin of Northern China. Hydrological Processes 33, 1075–1088. https://doi.org/10.1002/hyp.13386

Jr, R.R.H., n.d. A Review of Twentieth- Century Drought Indices Used in the United States 18.

Lan, T., Zhang, H., Xu, C., Singh, V.P., Lin, K., 2020. Detection and attribution of abrupt shift in minor periods in human-impacted streamflow. Journal of Hydrology 584, 124637. https://doi.org/10.1016/j.jhydrol.2020.124637

Li, J.Z., Wang, Y.X., Li, S.F., Hu, R., 2015. A Nonstationary Standardized Precipitation Index incorporating climate indices as covariates. J. Geophys. Res. Atmos. 120. https://doi.org/10.1002/2015JD023920

Li, Y., Gong, Y., Huang, C., 2021. Construction of combined drought index based on bivariate joint distribution. Alexandria Engineering Journal 60, 2825–2833. https://doi.org/10.1016/j.aej.2021.01.006

Liu, M., Xu, X., Xu, C., Sun, A.Y., Wang, K., Scanlon, B.R., Zhang, L., 2017. A new drought index that considers the joint effects of climate and land surface change: A NEW DROUGHT INDEX. Water Resour. Res. 53, 3262–3278. https://doi.org/10.1002/2016WR020178

McKee, T.B., Doesken, N.J., Kleist, J., n.d. THE RELATIONSHIP OF DROUGHT FREQUENCY AND DURATION TO TIME SCALES 6.

Mekonnen, M.M., Hoekstra, A.Y., 2016. Four billion people facing severe water scarcity. Sci. Adv. 2, e1500323. https://doi.org/10.1126/sciadv.1500323

Mishra, A.K., Singh, V.P., 2010. A review of drought concepts. Journal of Hydrology 391, 202–216. https://doi.org/10.1016/j.jhydrol.2010.07.012

Mishra, V., Smoliak, B.V., Lettenmaier, D.P., Wallace, J.M., 2012. A prominent pattern of year-to-year variability in Indian Summer Monsoon Rainfall. Proc. Natl. Acad. Sci. U.S.A. 109, 7213–7217. https://doi.org/10.1073/pnas.1119150109

Ndehedehe, C.E., Anyah, R.O., Alsdorf, D., Agutu, N.O., Ferreira, V.G., 2019. Modelling the impacts of global multi-scale climatic drivers on hydro-climatic extremes (1901–2014) over the Congo basin. Science of The Total Environment 651, 1569–1587. https://doi.org/10.1016/j.scitotenv.2018.09.203

Park, J., Sung, J.H., Lim, Y.-J., Kang, H.-S., 2019. Introduction and application of non-stationary standardized precipitation index considering probability distribution function and return period. Theor Appl Climatol 136, 529–542. https://doi.org/10.1007/s00704-018-2500-y

Rajsekhar, D., Singh, Vijay.P., Mishra, Ashok.K., 2015. Multivariate drought index: An information theory based approach for integrated drought assessment. Journal of Hydrology 526, 164–182. https://doi.org/10.1016/j.jhydrol.2014.11.031

Rana, S., McGregor, J., Renwick, J., 2015. Precipitation Seasonality over the Indian Subcontinent: An Evaluation of Gauge, Reanalyses, and Satellite Retrievals. Journal of Hydrometeorology 16, 631–651. https://doi.org/10.1175/JHM-D-14-0106.1

Rashid, Md.M., Beecham, S., 2019. Development of a non-stationary Standardized Precipitation Index and its application to a South Australian climate. Science of The Total Environment 657, 882–892. https://doi.org/10.1016/j.scitotenv.2018.12.052

Rigby, R.A., Stasinopoulos, D.M., 2005. Generalized Additive Models for Location, Scale and Shape. Journal of the Royal Statistical Society. Series C (Applied Statistics) 54, 507–554.

Shah, D., Mishra, V., 2020. Integrated Drought Index (IDI) for Drought Monitoring and Assessment in India. Water Resour. Res. 56. https://doi.org/10.1029/2019WR026284

Shao, S., Zhang, H., Singh, V.P., Ding, H., Zhang, J., Wu, Y., 2022. Nonstationary analysis of hydrological drought index in a coupled human-water system: Application of the GAMLSS with meteorological and anthropogenic covariates in the Wuding River basin, China. Journal of Hydrology 608, 127692. https://doi.org/10.1016/j.jhydrol.2022.127692

Sheffield, J., Wood, E.F., Roderick, M.L., 2012. Little change in global drought over the past 60 years. Nature 491, 435–438. https://doi.org/10.1038/nature11575

Shukla, S., Wood, A.W., 2008. Use of a standardized runoff index for characterizing hydrologic drought. Geophys. Res. Lett. 35, L02405. https://doi.org/10.1029/2007GL032487

Song, Z., Xia, J., She, D., Zhang, L., Hu, C., Zhao, L., 2020. The development of a Nonstationary Standardized Precipitation Index using climate covariates: A case study in the middle and lower reaches of Yangtze River Basin, China. Journal of Hydrology 588, 125115. https://doi.org/10.1016/j.jhydrol.2020.125115

Strupczewski, W.G., Singh, V.P., Feluch, W., 2001. Non-stationary approach to at-site ¯ood frequency modelling I. Maximum likelihood estimation. Journal of Hydrology 20.

Su, C., Chen, X., 2019. Assessing the effects of reservoirs on extreme flows using nonstationary flood frequency models with the modified reservoir index as a covariate. Advances in Water Resources 124, 29–40. https://doi.org/10.1016/j.advwatres.2018.12.004

Svensson, C., Hannaford, J., Prosdocimi, I., 2017. Statistical distributions for monthly aggregations of precipitation and streamflow in drought indicator applications. Water Resour. Res. 53, 999–1018. https://doi.org/10.1002/2016WR019276

Thorslund, J., Van Vliet, M.T.H., 2020. A global dataset of surface water and groundwater salinity measurements from 1980–2019. Sci Data 7, 231. https://doi.org/10.1038/s41597-020-0562-z

Van Loon, A.F., Ploum, S.W., Parajka, J., Fleig, A.K., Garnier, E., Laaha, G., Van Lanen, H.A.J., 2015. Hydrological drought types in cold climates: quantitative analysis of causing factors and qualitative survey of impacts. Hydrol. Earth Syst. Sci. 19, 1993–2016. https://doi.org/10.5194/hess-19-1993-2015

Van Loon, A.F., Van Lanen, H.A.J., 2013. Making the distinction between water scarcity and drought using an observation-modeling framework: DISTINGUISHING BETWEEN WATER SCARCITY AND DROUGHT. Water Resour. Res. 49, 1483–1502. https://doi.org/10.1002/wrcr.20147

Wang, F., Wang, Z., Yang, H., Di, D., Zhao, Y., Liang, Q., Hussain, Z., 2020. Comprehensive evaluation of hydrological drought and its relationships with meteorological drought in the Yellow River basin, China. Journal of Hydrology 584, 124751. https://doi.org/10.1016/j.jhydrol.2020.124751

Wang, G., Li, J., Sun, W., Xue, B., A, Y., Liu, T., 2019. Non-point source pollution risks in a drinking water protection zone based on remote sensing data embedded within a nutrient budget model. Water Research 157, 238–246. https://doi.org/10.1016/j.watres.2019.03.070

Wang, H., Chen, Y., Pan, Y., Li, W., 2015. Spatial and temporal variability of drought in the arid region of China and its relationships to teleconnection indices. Journal of Hydrology 523, 283–296. https://doi.org/10.1016/j.jhydrol.2015.01.055

Wang, Y., Duan, L., Liu, T., Li, J., Feng, P., 2020. A Non-stationary Standardized Streamflow Index for hydrological drought using climate and human-induced indices as covariates. Science of The Total Environment 699, 134278. https://doi.org/10.1016/j.scitotenv.2019.134278

Wilhite, D.A., Glantz, M.H., 1985. Understanding: the Drought Phenomenon: The Role of Definitions. Water International 10, 111–120. https://doi.org/10.1080/02508068508686328

Won, J., Choi, J., Lee, O., Kim, S., 2020. Copula-based Joint Drought Index using SPI and EDDI and its application to climate change. Science of The Total Environment 744, 140701. https://doi.org/10.1016/j.scitotenv.2020.140701

Wu, J., Chen, Xingwei, Love, C.A., Yao, H., Chen, Xiaohong, AghaKouchak, A., 2020. Determination of water required to recover from hydrological drought: Perspective from drought propagation and non-standardized indices. Journal of Hydrology 590, 125227. https://doi.org/10.1016/j.jhydrol.2020.125227

Yin, J., Zhan, X., Hain, C.R., Liu, J., Anderson, M.C., 2018. A Method for Objectively Integrating Soil Moisture Satellite Observations and Model Simulations Toward a Blended Drought Index. Water Resour. Res. 54, 6772–6791. https://doi.org/10.1029/2017WR021959

Yu, H., Li, T., Liu, P., 2019. Influence of ENSO on frequency of wintertime fog days in Eastern China. Clim Dyn 52, 5099–5113. https://doi.org/10.1007/s00382-018-4437-3

Yu, S., Qin, H., Ding, W., 2023. Modeling the effects of vegetation dynamics on the hydrological performance of a bioretention system. Journal of Hydrology 620, 129473. https://doi.org/10.1016/j.jhydrol.2023.129473

Yuan, N., Fu, Z., Zhang, H., Piao, L., Xoplaki, E., Luterbacher, J., 2015. Detrended Partial-Cross-Correlation Analysis: A New Method for Analyzing Correlations in Complex System. Sci Rep 5, 8143. https://doi.org/10.1038/srep08143

Zargar, A., Sadiq, R., Naser, B., Khan, F.I., 2011. A review of drought indices. Environ. Rev. 19, 333–349. https://doi.org/10.1139/a11-013

Zhang, A., Zhang, C., Fu, G., Wang, B., Bao, Z., Zheng, H., 2012. Assessments of Impacts of Climate Change and Human Activities on Runoff with SWAT for the Huifa River Basin, Northeast China. Water Resour Manage 26, 2199–2217. https://doi.org/10.1007/s11269-012-0010-8

Zhang, D., Zhang, Q., Qiu, J., Bai, P., Liang, K., Li, X., 2018. Intensification of hydrological drought due to human activity in the middle reaches of the Yangtze River, China. Science of The Total Environment 637–638, 1432–1442. https://doi.org/10.1016/j.scitotenv.2018.05.121

Zhang, T., Su, X., Feng, K., 2021. The development of a novel nonstationary meteorological and hydrological drought index using the climatic and anthropogenic indices as covariates. Science of The Total Environment 786, 147385. https://doi.org/10.1016/j.scitotenv.2021.147385

Zhao, S., Cong, D., He, K., Yang, H., Qin, Z., 2017. Spatial-Temporal Variation of Drought in China from 1982 to 2010 Based on a modified Temperature Vegetation Drought Index (mTVDI). Sci Rep 7, 17473. https://doi.org/10.1038/s41598-017-17810-3

Table 1. Classification of four models.

Model	Description	μ	σ
0	Stationary	~1	~1
1	Nonstationary	~1	~ covariate
2	Nonstationary	~covariate	~1
3	Nonstationary	~ covariate	~covariate

Table 2. The threshold values and descriptions of the NIDI in this study.

Description	Values
Extreme drought	<-2.00
Serious drought	-1.50 to -1.99
Moderate drought	-1.00 to -1.49
No drought	>-1.00

Table 3. Results of the time-varying vine copula function.

tree	edge	copula	MLE		GA	
			par	AIC	par	AIC
1	3,2	Gumbel copula	3.1969	-881.14	3.1938	**-881.88**
	1,3	Normal copula	0.5142	-171.63	0.5147	**-171.93**
	4,1	Normal copula	0.6582	-331.21	0.6583	**-331.30**
2	1,2;3	Frank copula	0.3350	0.16	0.3415	**0.18**
	4,3;1	Normal copula	0.1306	-7.67	0.1354	**-7.85**
3	4,2;1,3	Joe copula	-0.6320	-14.42	-0.6215	**-14.89**

Figure 1

Click here to access/download;Figure;Figure 1.tif

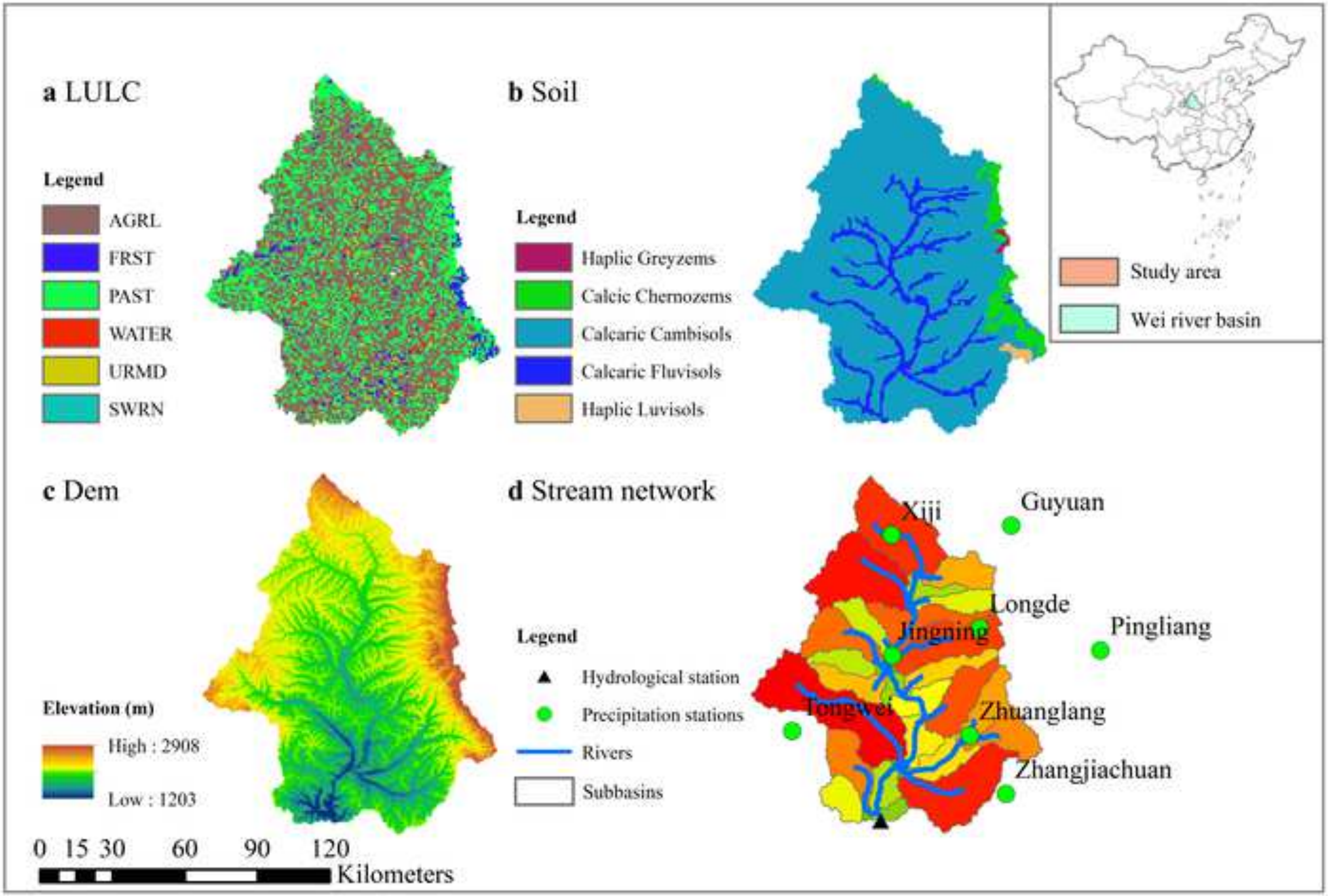

Figure 2

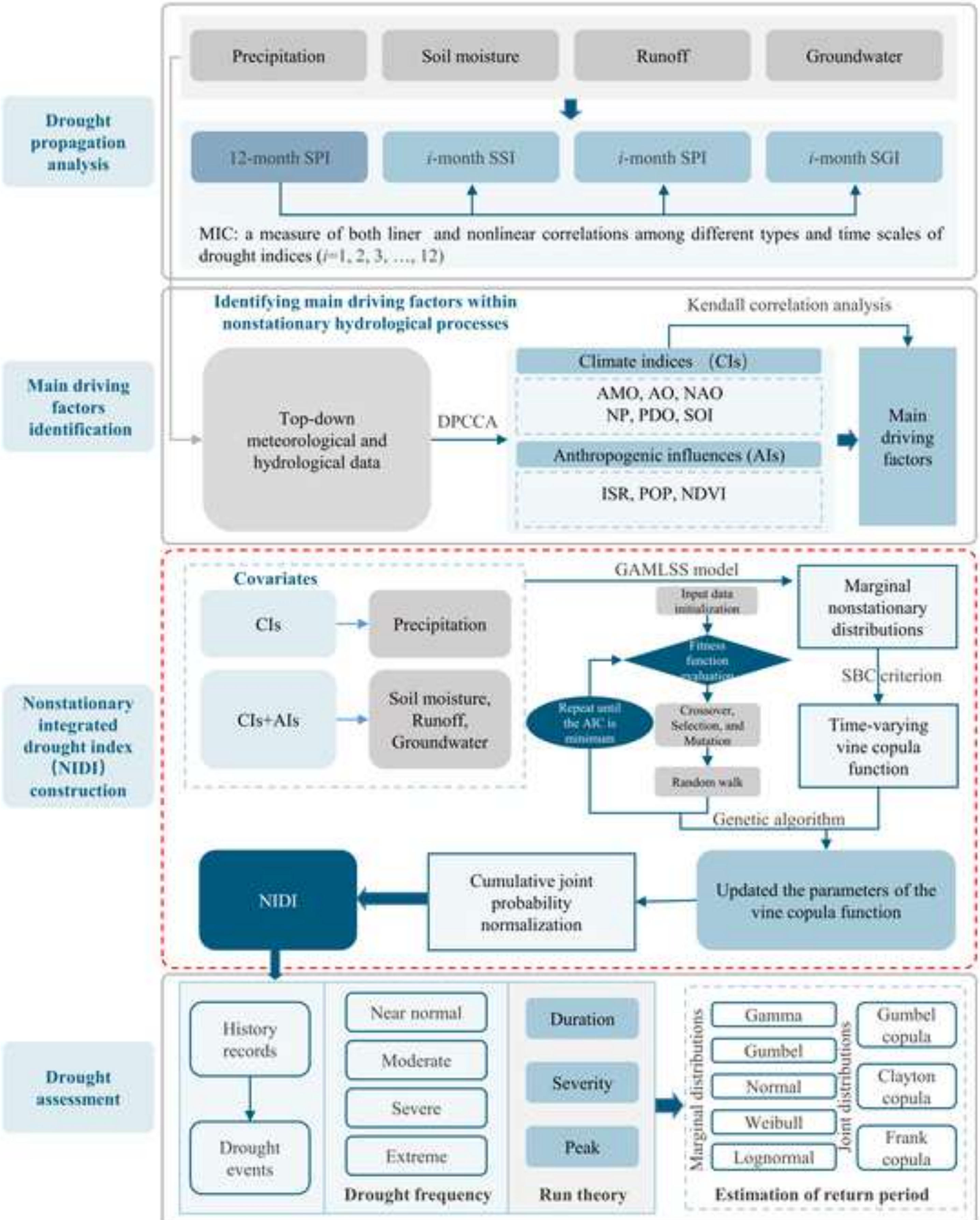
Drought propagation analysis
Precipitation
Soil moisture
Runoff
Groundwater
12-month SPI
i-month SSI
i-month SPI
i-month SGI
MIC: a measure of both liner and nonlinear correlations among different types and time scales of drought indices (i=1, 2, 3, …, 12)
Main driving factors identification
Identifying main driving factors within nonstationary hydrological processes
Kendall correlation analysis
Top-down meteorological and hydrological data
DPCCA
Climate indices (CIs)
AMO, AO, NAO
NP, PDO, SOI
Anthropogenic influences (AIs)
ISR, POP, NDVI
Main driving factors
Nonstationary integrated drought index (NIDI) construction
Covariates
CIs
Precipitation
CIs+AIs
Soil moisture, Runoff, Groundwater
GAMLSS model
Input data initialization
Fitness function evaluation
Repeat until the AIC is minimum
Crossover, Selection, and Mutation
Random walk
Genetic algorithm
Marginal nonstationary distributions
SBC criterion
Time-varying vine copula function
Updated the parameters of the vine copula function
Cumulative joint probability normalization
NIDI
Drought assessment
History records
Drought events
Near normal
Moderate
Severe
Extreme
Drought frequency
Duration
Severity
Peak
Run theory
Marginal distributions
Gamma
Gumbel
Normal
Weibull
Lognormal
Joint distributions
Gumbel copula
Clayton copula
Frank copula
Estimation of return period

Figure 3

Click here to access/download;Figure;Figure 3.tif

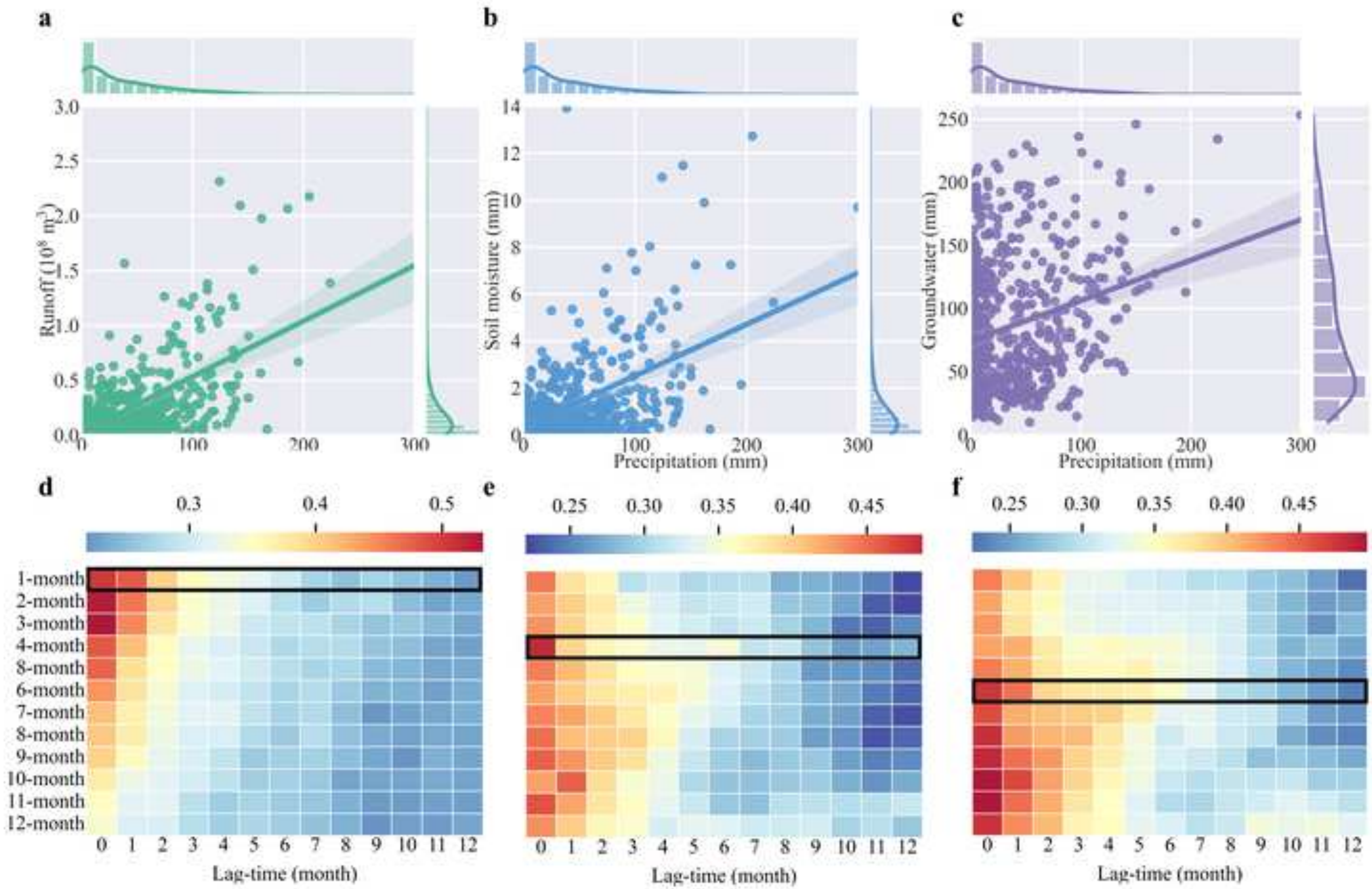

Figure 4 Click here to access/download;Figure;Figure 4.tif

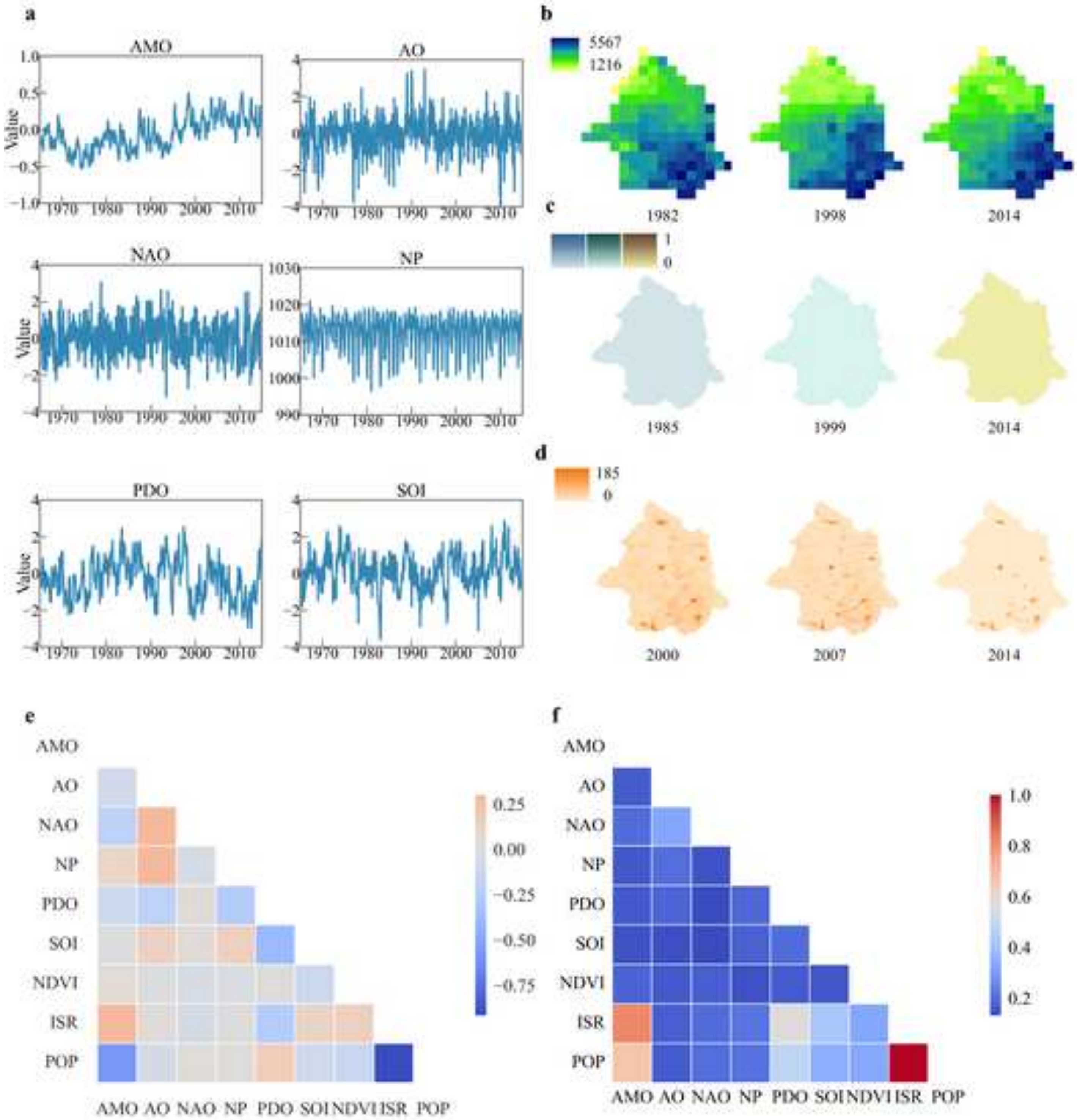

Figure 5

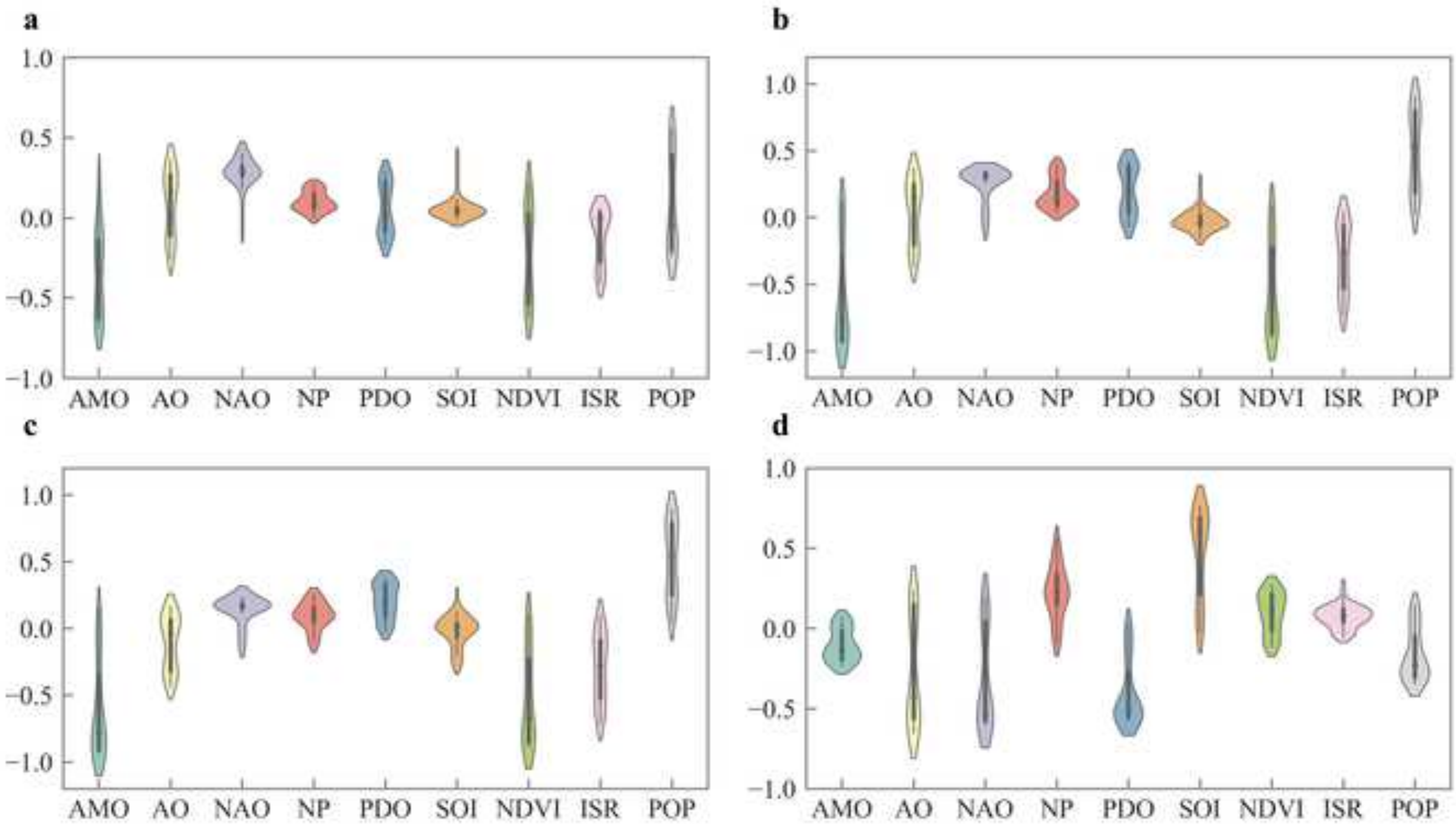
a
1.0
0.5
0.0
−0.5
−1.0
AMO AO NAO NP PDO SOI NDVI ISR POP
b
1.0
0.5
0.0
−0.5
−1.0
AMO AO NAO NP PDO SOI NDVI ISR POP
c
1.0
0.5
0.0
−0.5
−1.0
AMO AO NAO NP PDO SOI NDVI ISR POP
d
1.0
0.5
0.0
−0.5
−1.0
AMO AO NAO NP PDO SOI NDVI ISR POP

Figure 6

Click here to access/download;Figure;Figure 6.tif

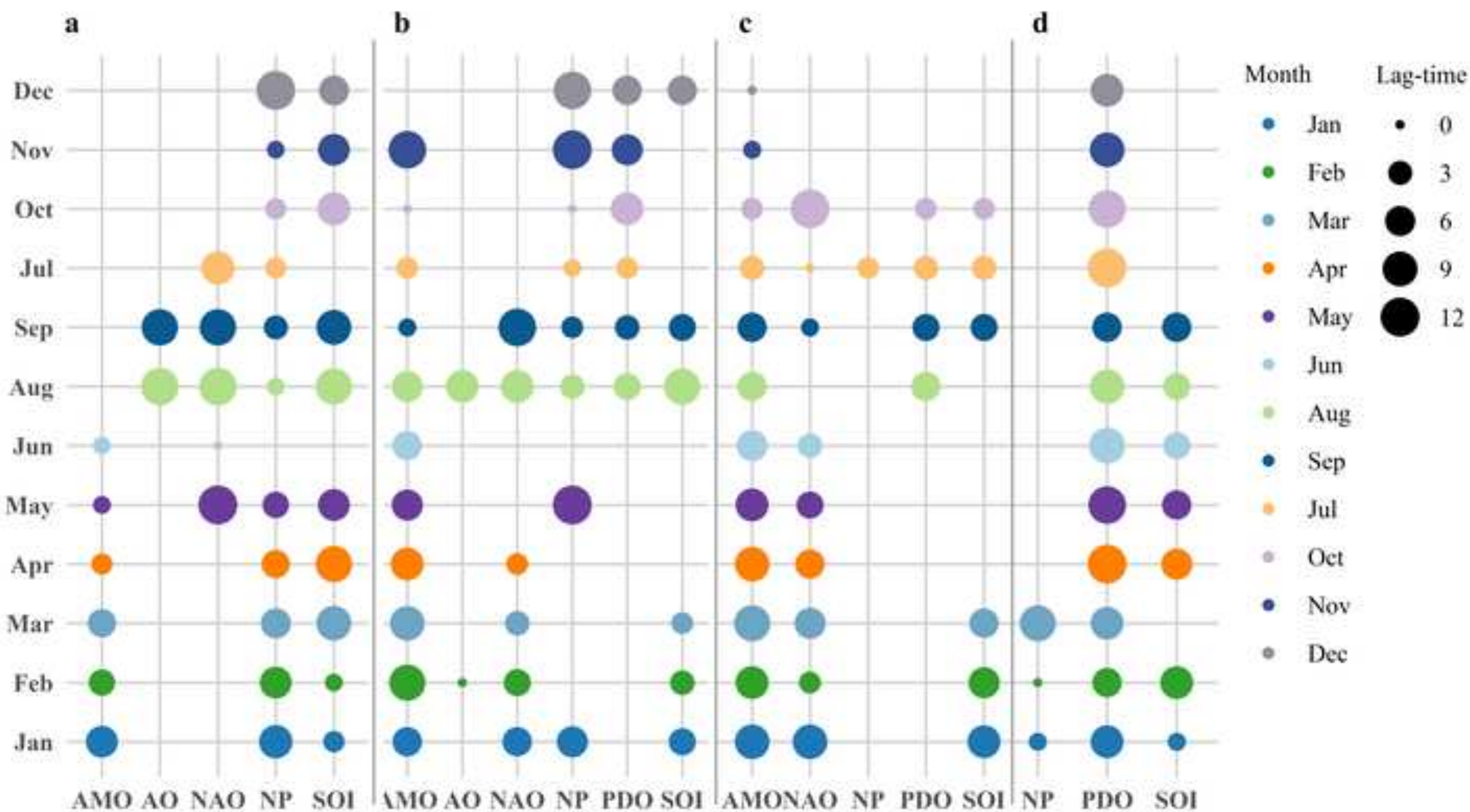

Figure 7 Click here to access/download;Figure;Figure 7.tif

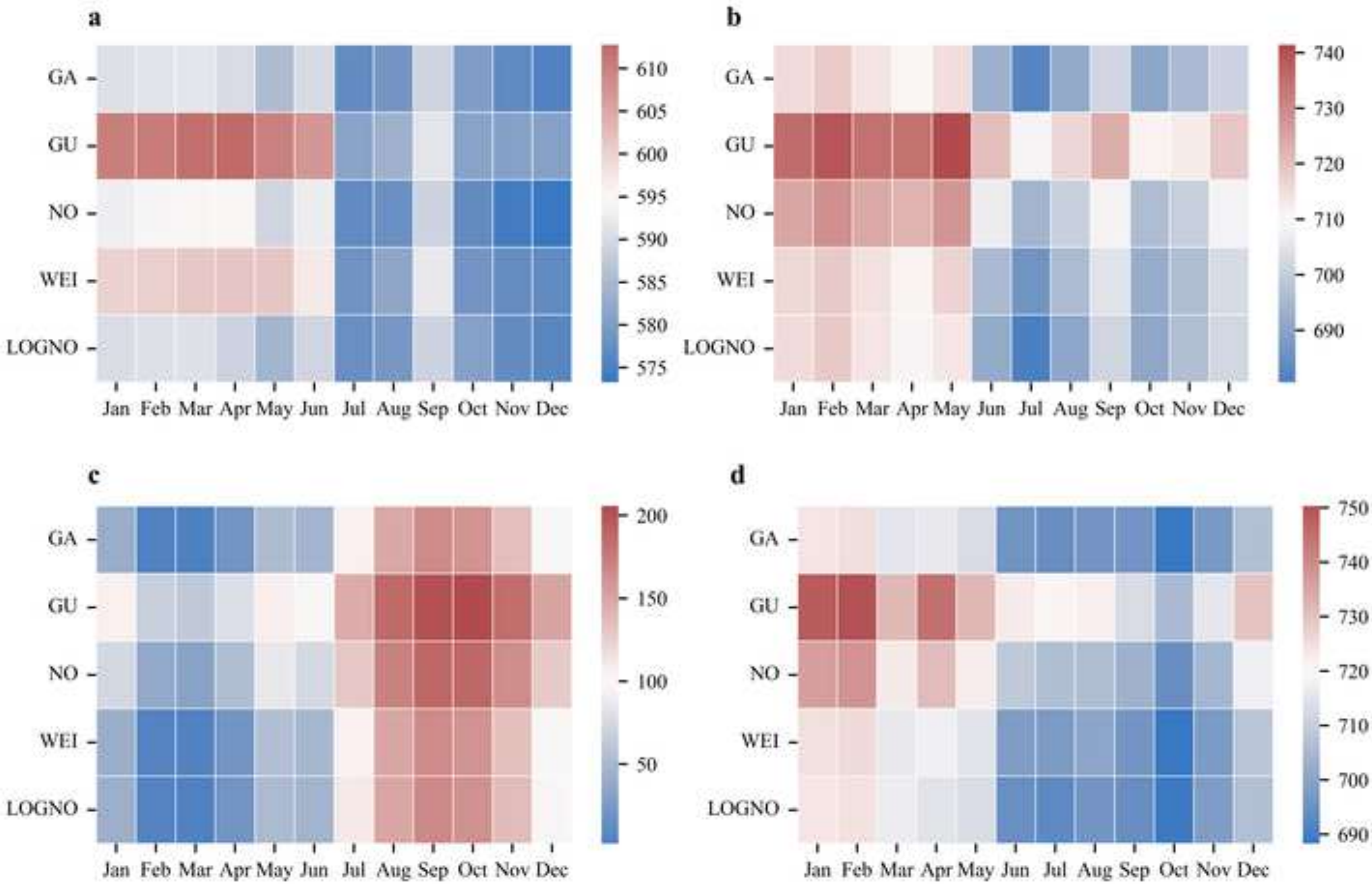

Figure 8

Click here to access/download;Figure;Figure 8.tif

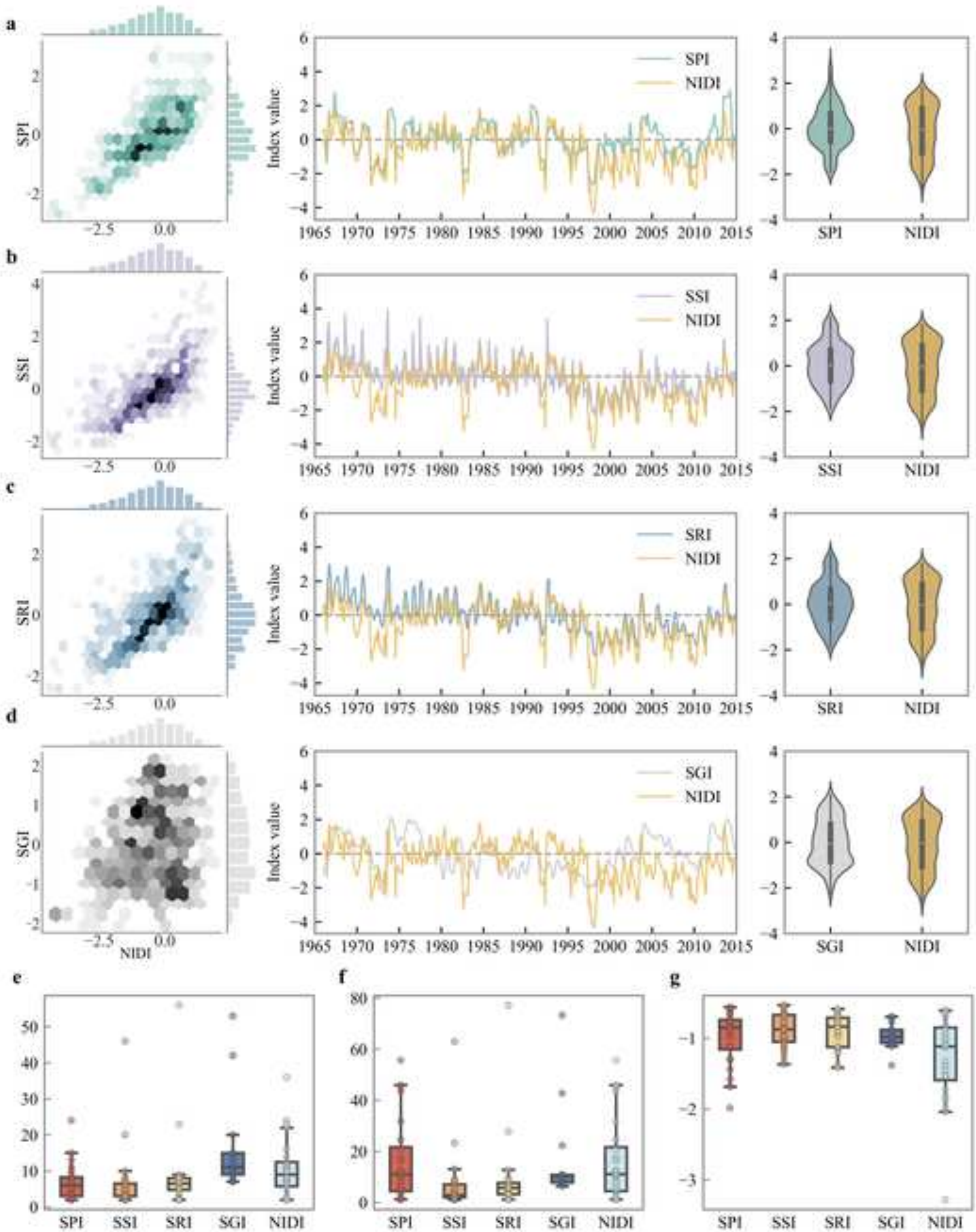

Figure 9

Click here to access/download;Figure;Figure 9.tif

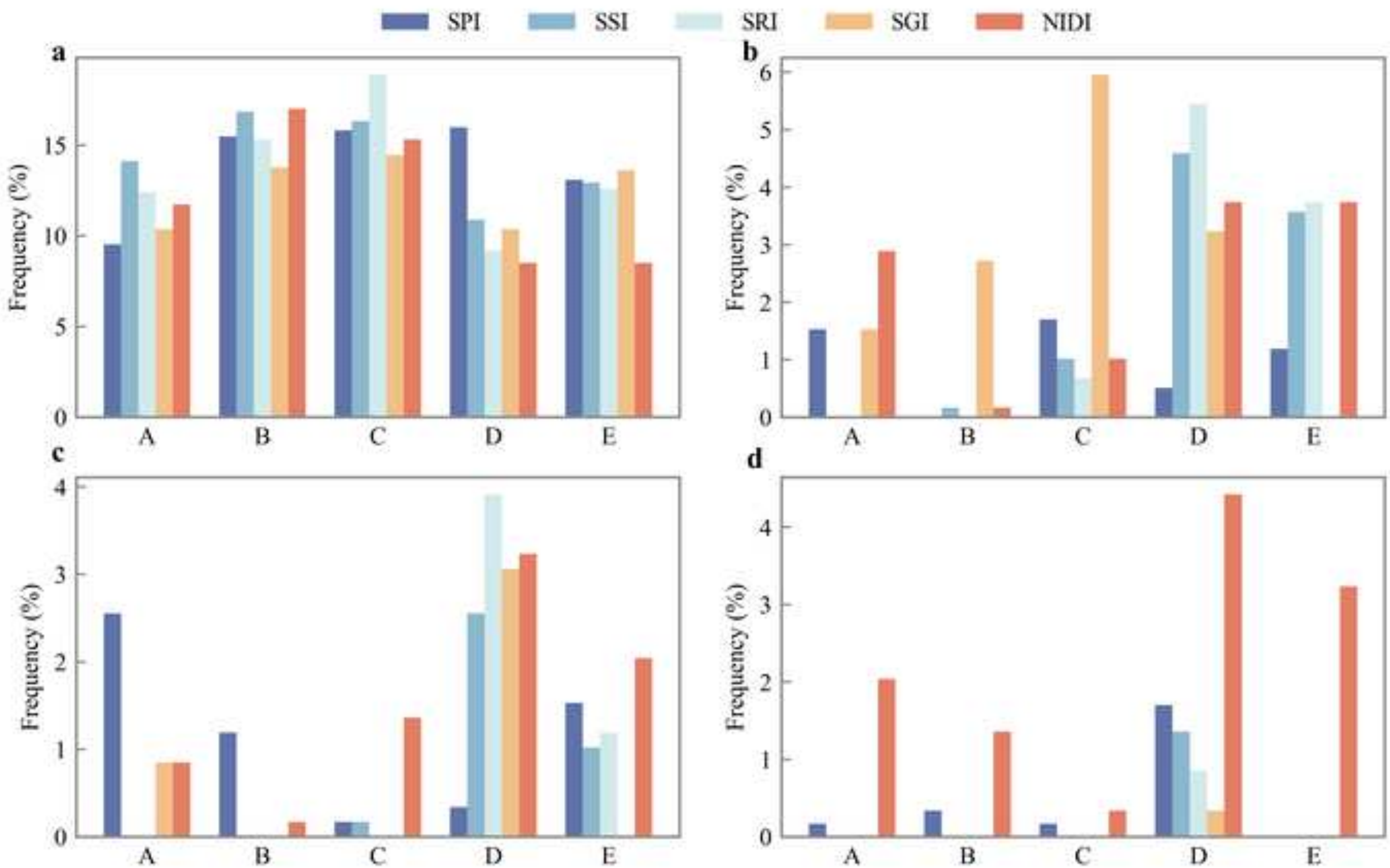

Figure 10

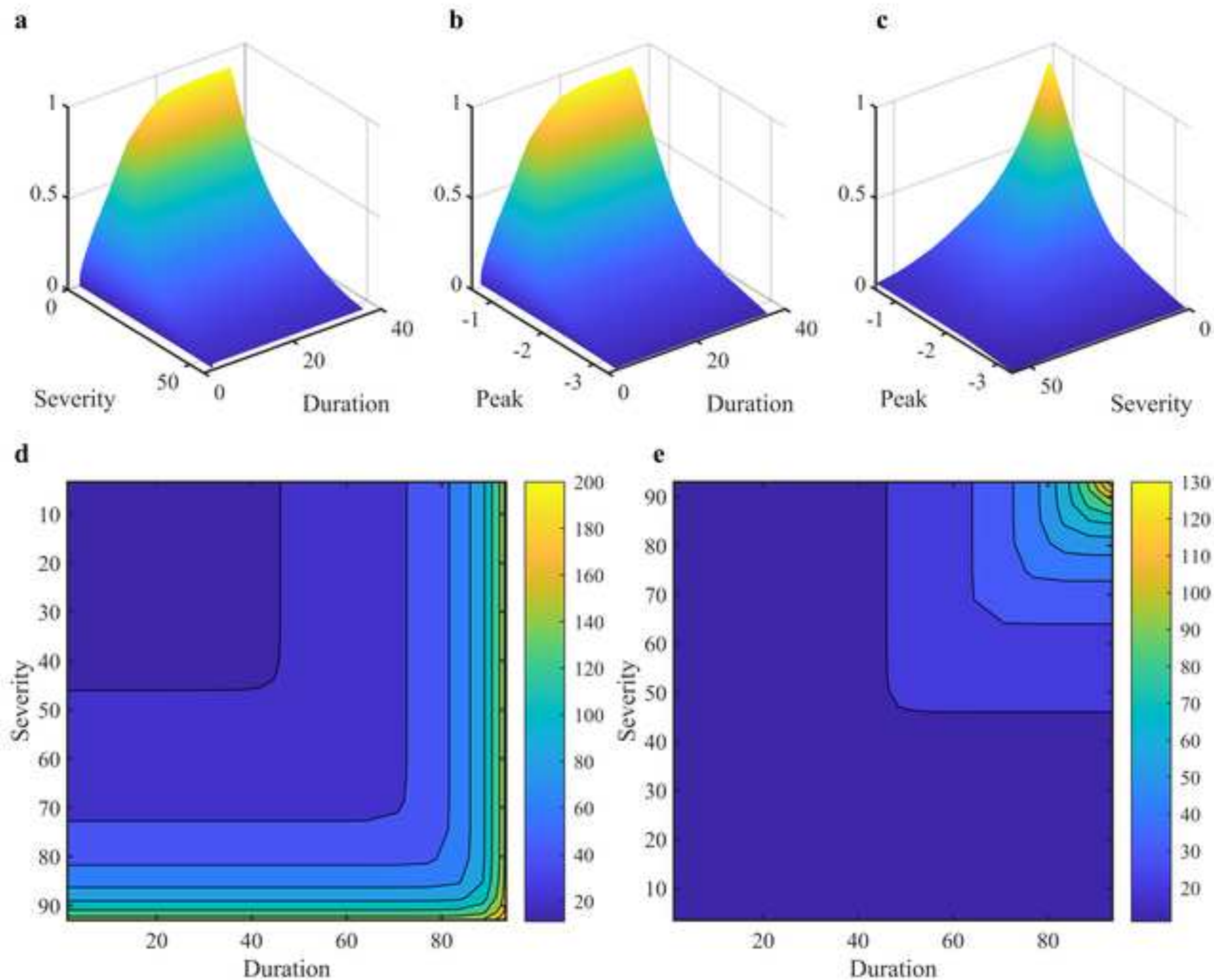
a
1
0.5
0
0
50
Severity
0
20
40
Duration
b
1
0.5
0
-1
-2
-3
Peak
0
20
40
Duration
c
1
0.5
0
-1
-2
-3
Peak
50
0
Severity
d
10
20
30
40
50
60
70
80
90
Severity
20
40
60
80
Duration
200
180
160
140
120
100
80
60
40
20
e
90
80
70
60
50
40
30
20
10
Severity
20
40
60
80
Duration
130
120
110
100
90
80
70
60
50
40
30
20

We confirm that this work is original and has not been published elsewhere, nor is it currently under consideration for publication elsewhere. All authors have read and approved the manuscript being submitted, and agree to its submittal to this journal, and have no conflicts of interest to disclose.

The work described in this paper was supported financially by the National Natural Science Foundation of China (NSFC) (Grant No. 52179005 and No. 52209006).